

Three Lectures On Topological Phases Of Matter

Edward Witten

School of Natural Sciences, Institute for Advanced Study, Princeton, NJ 08540

Abstract

These notes are based on lectures at the PSSCMP/PiTP summer school that was held at Princeton University and the Institute for Advanced Study in July, 2015. They are devoted largely to topological phases of matter that can be understood in terms of free fermions and band theory. They also contain an introduction to the fractional quantum Hall effect from the point of view of effective field theory.

Contents

0	Introduction	2
1	Lecture One	3
1.1	Relativistic Dispersion In One Space Dimension	3
1.2	Three Dimensions	5
1.3	The Nielsen-Ninomiya Theorem	8
1.4	The Berry Connection	11
1.5	Some Examples	13
1.6	Band Crossing At The Fermi Energy	14
1.7	Including Spin	15
1.8	A System With Many Bands	16
1.9	Two Dimensions	18
1.10	Weyl Fermions And Fermi Arcs	20
1.11	Gapless Boundary Modes From Dirac Fermions	24
1.12	Discrete Lattice Symmetries and Massless Dirac Fermions	26
1.13	Simple Examples Of Band Hamiltonians	29
2	Lecture Two	30
2.1	Chern-Simons Effective Action	30
2.2	Quantization Of The Chern-Simons Coupling	32
2.3	Quantization Of The Hall Conductivity	33
2.4	Relation To Band Topology	35
2.5	Proof Of The Equivalence	37
2.6	Edge States And Anomaly Inflow	40
2.7	The Charge Pump	41
2.8	Joining Valence And Conduction Bands	42
2.9	More On The Fractional Quantum Hall Effect	45
2.10	More On Fermi Arcs	45
3	Lecture Three	47
3.1	More On The Fractional Quantum Hall Effect	47
3.2	More On Edge States Of The Integer Quantum Hall Effect	53
3.3	Haldane's Model Of Graphene	56

0 Introduction

In recent years, a number of fascinating new applications of quantum field theory in condensed matter physics have been discovered. For an entrée to the literature, see the review articles [1, 2, 3] and the book [4].

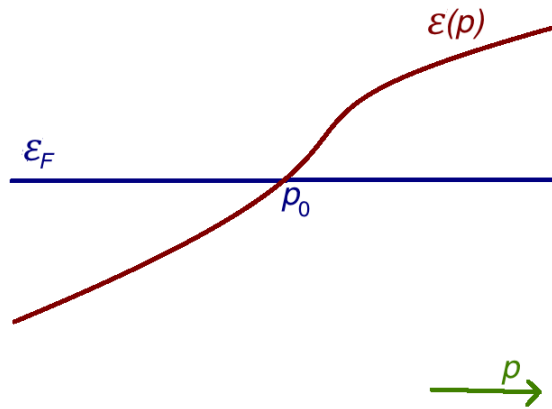


Figure 1: In one dimension, the single-particle energy $\varepsilon(p)$ generically crosses the Fermi energy at an isolated momentum p_0 .

The present notes are based on the first three of four lectures that I gave on these matters at the PSSCMP/PiTP summer school at Princeton University and the Institute for Advanced Study in July, 2015. These lectures contained very little novelty; I simply explained what I have been able to understand of a fascinating subject. (The fourth lecture did contain some novelty and has been written up separately [5].) The references include some classic recent and less recent papers, but they are certainly not complete.

In these lectures, I mostly concentrated on phases of matter that can be understood in terms of noninteracting electrons and topological band theory. The main exception was a short introduction to some aspects of the fractional quantum Hall effect.

These notes mostly follow the original lectures rather closely. Some topics have been slightly rearranged and a few matters for which unfortunately there was no time in the original lectures have been added. Some topics treated here were described from a different point of view by other lecturers at the school, especially Charlie Kane and Nick Read.

1 Lecture One

1.1 Relativistic Dispersion In One Space Dimension

We will start by asking under what conditions we should expect to find a relativistic dispersion relation for electrons in a crystal. In one space dimension, the answer is familiar. Writing $\varepsilon(p)$ for the single particle energy ε as a function of momentum p , generically $\varepsilon(p)$ crosses the Fermi energy with a nonzero slope at some $p = p_0$ (fig. 1).

Then linearizing the dispersion relation around $p = p_0$, we get

$$\varepsilon = \varepsilon(p_0) + v(p - p_0) + \mathcal{O}((p - p_0)^2), \quad v = \left. \frac{\partial \varepsilon}{\partial p} \right|_{p=p_0}. \quad (1.1)$$

Apart from the additive constant $\varepsilon(p_0)$ and the shift $p \rightarrow p - p_0$, this is a relativistic dispersion relation, analogous to $\varepsilon = cp$, with the speed of light c replaced by v . For $v > 0$ ($v < 0$), the gapless mode that lives near $p = p_0$ travels to the right (left).

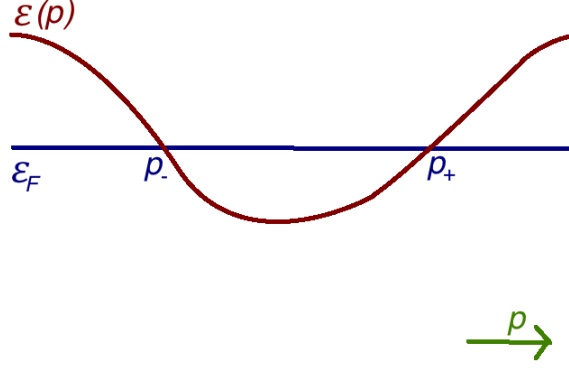


Figure 2: In one dimension, for every value of the momentum at which $\varepsilon(p)$ increases above ε_F , there is another point at which it decreases below ε_F .

The corresponding continuum model describing the modes near $p = p_0$ is

$$H = v \int_{-\infty}^{\infty} dx \psi^* \left(-i \frac{\partial}{\partial x} \right) \psi. \quad (1.2)$$

This is a relativistic action for a 1d chiral fermion, except that v appears instead of c and $-i\partial/\partial x$ represents $p - p_0$ instead of p . Also we have omitted from H the “constant” $\varepsilon(p_0)$ per particle:

$$\varepsilon(p_0) \int_{-\infty}^{\infty} dx \psi^* \psi. \quad (1.3)$$

This one-dimensional case gives an easy first example of how global conditions in topology constrain the possible low energy field theory that we can get – and how these constraints often mirror familiar facts about relativistic field theory and “anomalies.” We have to remember that in the context of a crystal, the momentum p is a periodic variable. Because $\varepsilon(p)$ is periodic, it follows (fig. 2) that for every time $\varepsilon(p)$ crosses the Fermi energy ε_F from below, there is another time that it crosses ε_F from above. So actually there are equally many gapless left-moving and right-moving fermion modes.

In relativistic terminology, the right-moving and left-moving modes are said to have positive and negative chirality. The motivation for this terminology is that the massless Dirac equation in 2 spacetime dimensions is

$$\left(\gamma^0 \frac{\partial}{\partial t} + \gamma^1 \frac{\partial}{\partial x} \right) \psi = 0, \quad (1.4)$$

where γ^μ are Dirac matrices, obeying the Clifford algebra relations

$$\{\gamma^\mu, \gamma^\nu\} = 2\eta^{\mu\nu}, \quad \eta_{\mu\nu} = \text{diag}(-1, 1). \quad (1.5)$$

In Hamiltonian form, the Dirac equation is

$$i \frac{\partial \psi}{\partial t} = -i \bar{\gamma} \frac{\partial \psi}{\partial x}, \quad (1.6)$$

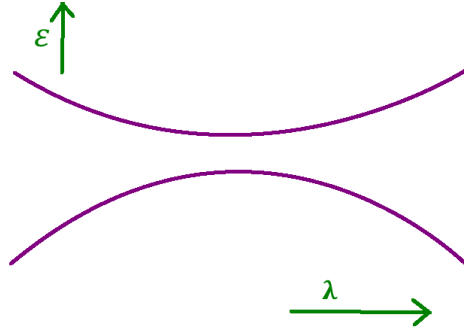


Figure 3: Generically, quantum mechanical energy levels do not cross as a parameter is varied.

where $\bar{\gamma} = \gamma_0\gamma_1$ (whose analog in 3+1 dimensions is usually called γ_5) is the “chirality operator.” So a fermion state of positive or negative chirality is right-moving or left-moving.

Thus a more realistic Hamiltonian for the gapless charged modes will be something like

$$H = -v_- \int_{-\infty}^{\infty} dx \psi_-^* \left(-i \frac{\partial}{\partial x} \right) \psi_- + v_+ \int_{-\infty}^{\infty} dx \psi_+^* \left(-i \frac{\partial}{\partial x} \right) \psi_+, \quad (1.7)$$

where ψ_+ and ψ_- are modes of positive and negative chirality, and in general they propagate with different velocities. If one is familiar with quantum gauge theories and anomalies, one will recognize that this topological fact – which is a 1d analog of the 3d Nielsen-Ninomiya theorem that we get to presently – has saved us from trouble. A purely 1 + 1-dimensional theory with, say, n_+ right-moving gapless electron modes and n_- left-moving ones is “anomalous,” meaning that it is not gauge-invariant and does not conserve electric charge – unless $n_+ = n_-$. The anomaly is the 1 + 1-dimensional version of the Adler-Bell-Jackiw anomaly [6, 7], which is very important in particle physics.

We can actually see the potential anomaly by re-examining fig. 2, but now assuming that a constant electric field is turned on. In the presence of an electric field with a sign such that $dp/dt > 0$ for each electron, the electrons will all “flow” to the right in the picture. This creates electrons at $p = p_+$ and holes at $p = p_-$, so the charge carried by the $p = p_+$ mode or by the $p = p_-$ mode is not conserved, although the total charge is conserved, of course. Thus charge conservation depends on having both types of mode equally.

1.2 Three Dimensions

There is certainly more that one could say in 1 space dimension, but instead we are going to go on to spatial dimension 3. As a preliminary, recall that quantum mechanical energy levels repel, which means that if $H(\lambda)$ is a generic 1-parameter family of Hamiltonians, depending on a parameter λ , and with no particular symmetry, then generically its energy levels do not cross as a function of λ (fig. 3). But [8] how much do levels repel each other? Generically, how many parameters do we have to adjust to make two energy levels coincide?

The answer to this question is that we have to adjust 3 real parameters, because a generic

2×2 Hermitian matrix depends on 4 real parameters

$$H = \begin{pmatrix} a & b \\ \bar{b} & c \end{pmatrix}, \quad (1.8)$$

but a 2×2 Hermitian matrix whose energy levels are equal depends on only 1 real parameter

$$H = \begin{pmatrix} a & 0 \\ 0 & a \end{pmatrix}. \quad (1.9)$$

To put this differently, any 2×2 Hermitian matrix is

$$H = a + \vec{b} \cdot \vec{\sigma}, \quad (1.10)$$

where $\vec{\sigma}$ are the Pauli matrices. The condition for H to have equal eigenvalues is $\vec{b} = 0$, and this is three real conditions.

In three dimensions, a band Hamiltonian $H(p_1, p_2, p_3)$ depends on three real parameters, so it is natural for two bands to cross at some isolated value $p = p_*$. Near $p = p_*$, and looking only at the two bands in question, the Hamiltonian looks something like

$$H = a(p) + \vec{b}(p) \cdot \vec{\sigma}, \quad (1.11)$$

where $\vec{b}(p) = 0$ at $p = p_*$. Expanding near $p = p_*$,

$$b_i(p) = \sum_j b_{ij}(p - p_*)_j + \mathcal{O}((p - p_*)^2), \quad b_{ij} = \left. \frac{\partial b_i}{\partial p_j} \right|_{p=p_*}. \quad (1.12)$$

Thus dropping a constant and ignoring higher order terms, the band splitting is described near $p = p_*$ by

$$H' = \sum_{i,j} \sigma_i b_{ij}(p - p_*)_j. \quad (1.13)$$

Apart from a shift $p \rightarrow p - p_*$, this is essentially a chiral Dirac Hamiltonian in $3 + 1$ dimensions. Let us review this fact. The massless Dirac equation in $3 + 1$ dimensions is

$$\sum_{\mu=0}^3 \gamma^\mu \partial_\mu \psi = 0, \quad \{\gamma^\mu, \gamma^\nu\} = 2\eta^{\mu\nu}, \quad \eta_{\mu\nu} = \text{diag}(-1, 1, 1, 1). \quad (1.14)$$

In Hamiltonian form, this equation is

$$i \frac{\partial \psi}{\partial t} = -i \sum_k \gamma_0 \gamma_k \frac{\partial \psi}{\partial x^k}. \quad (1.15)$$

To represent the four gamma matrices, we need 4×4 matrices (which can be chosen to be real). However, the matrix

$$\gamma_5 = i\gamma_0\gamma_1\gamma_2\gamma_3 \quad (1.16)$$

is Lorentz-invariant. It obeys $\gamma_5^2 = 1$, so its eigenvalues are ± 1 . We can place on ψ a ‘‘chirality condition’’ $\gamma_5 \psi = \pm \psi$, reducing to a 2×2 Dirac Hamiltonian. But then, because of the factor

of i in the definition of γ_5 , and in contrast to what happens in $1 + 1$ dimensions, the adjoint of ψ obeys the opposite chirality condition.

Once we reduce to a chiral 2×2 Dirac Hamiltonian with $\gamma_5\psi = \pm\psi$, the matrices $\gamma_0\gamma_i$ that appear in the Dirac Hamiltonian are 2×2 hermitian matrices and we can take them to be, up to sign, the Pauli sigma matrices

$$\sigma_i = \pm\gamma_0\gamma_i. \quad (1.17)$$

The point is that, if $\gamma_5\psi = \pm\psi$, then *in acting on* ψ ,

$$\sigma_i\sigma_j = \delta_{ij} + i\epsilon_{ijk}\sigma_k. \quad (1.18)$$

(One may prove this for $i = 1, j = 2$ from the explicit identity $\gamma_0\gamma_1\gamma_0\gamma_2 = i\gamma_0\gamma_3\gamma_5$. The general case then follows from rotation symmetry.)

So the Dirac Hamiltonian

$$H = -i \sum_k \gamma_0\gamma_k \frac{\partial}{\partial x^k} \quad (1.19)$$

becomes for a chiral fermion

$$H = \mp ic \sum_k \sigma^k \frac{\partial}{\partial x^k} = \pm c \vec{\sigma} \cdot \vec{p}. \quad (1.20)$$

The sign depends on the fermion chirality, which determines which sign we had to pick in eqn. (1.17). (I have restored c , the speed of light.) As a matter of terminology, a charged relativistic fermion of definite chirality – in other words, with a definite value of γ_5 – is called a Weyl fermion. The physical meaning of the eigenvalue of γ_5 is that it determines the fermion “helicity” (spin around the direction of motion). Note that “helicity” is only a Lorentz-invariant notion for a *massless* particle (which is never at rest in any Lorentz frame) and indeed our starting point was the massless Dirac equation. The *antiparticle* – which one can think of as a hole in the Dirac sea – has opposite helicity,¹ somewhat as it has opposite charge. The chiral Dirac Hamiltonian of eqn. (1.20) describes two bands with $E = \pm c|p|$ (fig. 4).

Thus, the chiral Dirac Hamiltonian basically coincides with the generic Hamiltonian (1.13) that we found for a 2×2 band crossing, with the replacement $cp_k \rightarrow \sum_j b_{kj}p_j$. This replacement means, of course, that the fermion modes near $p = p_*$ do not propagate at velocity c but much more slowly. Also, they do not necessarily propagate isotropically in the standard Euclidean metric on \mathbf{R}^3 . In general, the natural metric governing these modes is

$$\|p\|^2 = \sum_i \left(\sum_j b_{ij}p_j \right)^2.$$

In other words, the effective metric is

$$G^{ij} = \sum_k b^i_k b^j_k.$$

¹This happens because – in contrast to what happens in $1 + 1$ dimensions – if the γ^μ are real then the chirality operator γ_5 is imaginary. Accordingly ψ and its hermitian adjoint obey opposite chirality conditions. The basic example in particle physics is that, in the approximation in which they are massless, neutrinos and antineutrinos have opposite helicity.

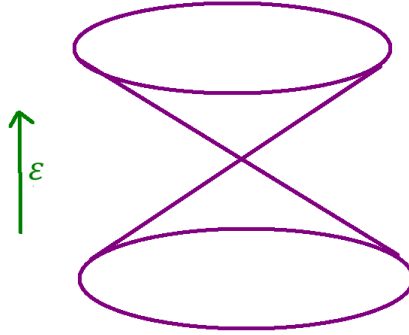


Figure 4: A pair of bands described by a chiral Dirac Hamiltonian.

Finally, and very importantly, the *chirality* of the gapless electron mode is given by

$$\text{sign det}(b_{ij}) = \text{sign det} \left(\frac{\partial b_i}{\partial p_j} \right) \Big|_{p=p_*}. \quad (1.21)$$

A gap crossing in which this determinant is positive (or negative) corresponds to a relativistic massless chiral fermion (or Weyl fermion) with $\gamma_5 = +1$ (or $\gamma_5 = -1$).

1.3 The Nielsen-Ninomiya Theorem

Now, however, we should remember something about relativistic quantum field theory in $3 + 1$ dimensions. A theory of a $U(1)$ gauge field (of electromagnetism) coupled to a massless chiral charged fermion of one chirality, with no counterpart of the opposite chirality, is anomalous: gauge invariance fails at the quantum level, and the theory is inconsistent. In $1 + 1$ dimensions, we avoided such a contradiction because of a simple topological fact that $\varepsilon(p)$ passes downward through the Fermi energy as often as it passes upwards, as in fig. 2. An analogous topological theorem saves the day in $3 + 1$ dimensions. This is the Nielsen-Ninomiya theorem [9, 10], which was originally formulated as an obstruction to a lattice regularization of relativistic chiral fermions.²

In formulating this theorem, we assume that the band Hamiltonian $H(p)$ is gapped except at finitely many isolated points in the Brillouin zone \mathcal{B} (fig. 5). We will attach an integer to each of these bad points, and show that these integers add up to 0.

To get started, we assume there are only two bands. Also, by simply subtracting a c -number function of p from $H(p)$, we can make $H(p)$ traceless, without changing the band crossings. So

$$H(p) = \vec{b}(p) \cdot \vec{\sigma}$$

for some vector-valued function $\vec{b}(p)$. Now away from the bad points, $\vec{b}(p) \neq 0$ and so we can define a unit vector

$$\vec{n}(p) = \frac{\vec{b}}{|\vec{b}|}.$$

²The Nielsen-Ninomiya theorem involves ideas somewhat analogous to those developed by Thouless, Kohmoto, Nightingale, and den Nijs [11] in celebrated work on the quantum Hall effect. We will describe their result in Lecture Two.

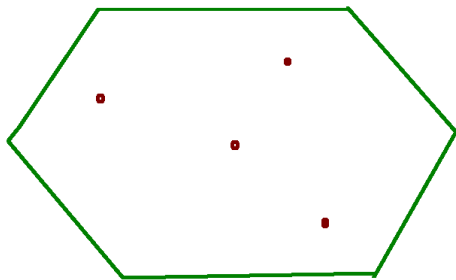


Figure 5: The interior of the hexagon symbolizes the Brillouin zone \mathcal{B} . We consider a band Hamiltonian that is gapped except at finitely many points, which are indicated by dots.

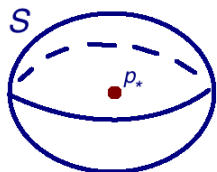


Figure 6: A small sphere S around a bad point p_* at which two levels cross.

The mapping $p \rightarrow \vec{n}(p)$ is defined away from the bad points. We want to understand its topological properties.

Let us consider just one of the bad points, say at $p = p_*$, and let S be a small sphere around this bad point (fig. 6). The map $p \rightarrow \vec{n}(p)$ is defined everywhere on S . This is a mapping from one two-sphere – namely S – to another two-sphere – parametrized by the unit vector \vec{n} . We will call that second two-sphere $S_{\vec{n}}$. In any dimension d , a continuous mapping from one d -dimensional sphere S^d to another sphere of the same dimension always has a “winding number” or “wrapping number,” the net number of times the first sphere wraps around the second. This reflects the fact that

$$\pi_d(S^d) \cong \mathbf{Z}.$$

Before developing any general theory, let us see what the winding number is in the case of the relativistic Dirac Hamiltonian $H = \pm \vec{\sigma} \cdot \vec{p}$, where the sign is the fermion chirality. For this Hamiltonian, $\vec{b} = \pm \vec{p}$, and hence $\vec{n} = \pm \vec{p}/|\vec{p}|$. The bad point is $\vec{p} = 0$, and we can take the sphere S that surrounds the bad point to be the unit sphere $|\vec{p}| = 1$. Thus the map from S to

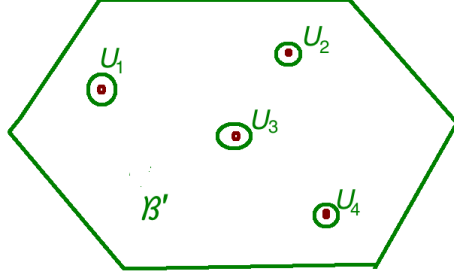


Figure 7: \mathcal{B}' is defined by removing a small open set U_α around each bad point p_α in the Brillouin zone.

$S_{\vec{n}}$ is just

$$\vec{n} = \pm \vec{p}. \quad (1.22)$$

This is the identity map, of winding number 1, in the case of + chirality, and it is minus the identity map, which winds around in reverse, with winding number -1 , in the case of $-$ chirality.

The Nielsen-Ninomiya theorem is the statement that the sum of the winding numbers at the bad points is always 0. Generically (in the absence of lattice symmetries that would lead to a more special behavior) a bad point of winding number bigger than 1 in absolute value will split into several bad points of winding number ± 1 . (We give in section 1.5 an explicit example of how this occurs.) So generically, the bad points all have winding numbers ± 1 , corresponding to gapless Weyl fermions of one chirality or the other. In this case, the vanishing of the sum of the winding numbers means that there are equally many gapless modes of positive or negative chirality, as a relativistic field theorist would expect for anomaly cancellation.

How does one prove that the sum of the winding numbers is 0? One rather down-to-earth method is as follows. The winding number for a map from S to $S_{\vec{n}}$ can be expressed as an integral formula:

$$w(S) = \frac{1}{4\pi} \int d^2p \epsilon^{\mu\nu} \vec{n} \cdot \partial_\mu \vec{n} \times \partial_\nu \vec{n}. \quad (1.23)$$

An equivalent way to write the same formula is

$$w(S) = \frac{1}{4\pi} \int_S d^2p \epsilon^{\mu\nu} \epsilon^{abc} n_a \frac{\partial n_b}{\partial p^\mu} \frac{\partial n_c}{\partial p^\nu}. \quad (1.24)$$

Now

$$0 = \partial_\lambda (\epsilon^{\lambda\mu\nu} \vec{n} \cdot \partial_\mu \vec{n} \times \partial_\nu \vec{n}), \quad (1.25)$$

since the right hand side is $\epsilon^{\lambda\mu\nu} \partial_\lambda \vec{n} \cdot \partial_\mu \vec{n} \times \partial_\nu \vec{n}$, which vanishes because it is the triple cross product of three vectors $\partial_\lambda \vec{n}$, $\partial_\mu \vec{n}$, and $\partial_\nu \vec{n}$ that are all normal to the sphere $|\vec{n}| = 1$.

For each bad point p_α , let U_α be a small open ball around p_α whose boundary is a sphere S_α . Let \mathcal{B} be the full Brillouin zone, and let \mathcal{B}' be what we get by removing from \mathcal{B} all of the U_α . Thus the boundary of \mathcal{B}' is $\partial\mathcal{B}' = \cup_\alpha S_\alpha$ (fig. 7). Then from Stokes's theorem,

$$0 = \frac{1}{4\pi} \int_{\mathcal{B}'} d^3p \partial_\lambda (\epsilon^{\lambda\mu\nu} (n \cdot \partial_\mu n \times \partial_\nu n))$$

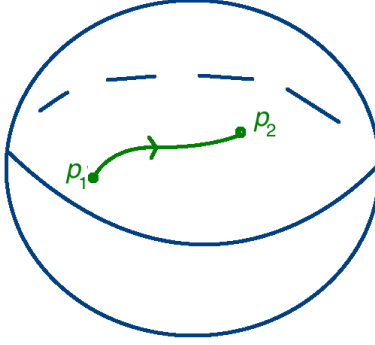


Figure 8: Transporting a quantum wavefunction over a path in some parameter space. One can think of the parameter space as a sphere that surrounds a bad point in the Brillouin zone.

$$\begin{aligned}
 &= \sum_{\alpha} \frac{1}{4\pi} \int_{S_{\alpha}} d^2p \epsilon^{\mu\nu} \vec{n} \cdot \partial_{\mu} \vec{n} \times \partial_{\nu} \vec{n} \\
 &= \sum_{\alpha} w(S_{\alpha}).
 \end{aligned}$$

Thus the sum of the winding numbers at bad points is 0, as promised.

In terms of differential forms, one can express this argument more briefly as follows. Let η be the volume form of $S_{\vec{n}}$. Thus, η is a closed 2-form whose integral is 1:

$$0 = d\eta, \quad \int_{S_{\vec{n}}} \eta = 1. \quad (1.26)$$

Given a map $\varphi : S \rightarrow S_{\vec{n}}$, the corresponding winding number is

$$w(S) = \int_S \varphi^*(\eta). \quad (1.27)$$

So

$$0 = \int_{B'} \varphi^*(d\eta) = \int_{B'} d\varphi^*(\eta) = \sum_{\alpha} \int_{S_{\alpha}} \varphi^*(\eta) = \sum_{\alpha} w(S_{\alpha}). \quad (1.28)$$

1.4 The Berry Connection

Another approach to the same result involves the *Berry connection*, and more fundamentally the line bundle on which the Berry connection is a connection. This approach is useful in generalizations. For each value of p away from the bad points, the Hamiltonian $H(p)$ has one negative eigenvalue, so the space of filled fermion states of momentum p is a 1-dimensional complex vector space that I will call \mathcal{L}_p . The fancy way to describe this situation is to say that as p varies, \mathcal{L}_p varies as the fiber of a complex line bundle \mathcal{L} over the Brillouin zone \mathcal{B} . A vector in \mathcal{L}_p is a wave function ψ_p that obeys $H(p)\psi_p = -\psi_p$. We can ask for ψ_p to be normalized, $\langle \psi_p, \psi_p \rangle = 1$, but there is no natural way to fix the *phase* of ψ_p .

However, suppose that we vary p continuously by a path $p = p(s)$ from, say, p_1 to p_2 , as indicated in fig. 8. For example, we can consider a path that lies in a sphere $|p - p_*| = \epsilon$

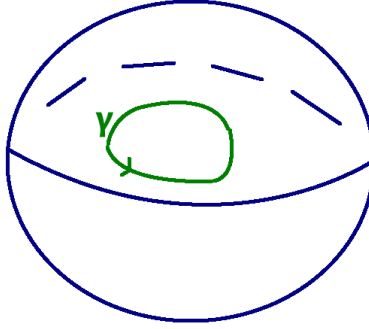


Figure 9: Parallel transport of a wavefunction around a closed loop.

around a bad point p_* . If we make any arbitrary choice of the phase of ψ_p at $p = p_1$, then we can parallel transport the phase of ψ_p along the given path by requiring that at all p along the path

$$\langle \psi_p, \frac{d}{ds} \psi_p \rangle = 0. \quad (1.29)$$

Concretely, the real part of this equation ensures that $\langle \psi_p, \psi_p \rangle$ is constant along the path, and the imaginary part of the equation determines how the phase of ψ_p depends on the parameter s .

Having a rule of parallel transport of the phase of ψ_p along any path amounts to defining a *connection* on \mathcal{B}' (more exactly on the line bundle $\mathcal{L} \rightarrow \mathcal{B}'$ whose sections we are parallel transporting). A *connection* on a complex line bundle \mathcal{L} is the same as an abelian gauge field, which we will call \mathcal{A} . Parallel transport around a closed loop γ using the Berry connection does not bring us back to the starting point (fig. 9). That is, the Berry connection is not flat; it has a curvature $\mathcal{F} = d\mathcal{A}$. This curvature, divided by 2π , represents (modulo torsion) the *first Chern class* of the line bundle $\mathcal{L} \rightarrow \mathcal{B}'$:

$$c_1(\mathcal{L}) \longleftrightarrow \frac{\mathcal{F}}{2\pi}. \quad (1.30)$$

If p_α is one of the bad points at which two bands cross and S_α is a small sphere around p_α , then the flux of $\mathcal{F}/2\pi$ over the sphere S_α is the winding number, as defined earlier:

$$w_\alpha(S) = \int_{S_\alpha} \frac{\mathcal{F}}{2\pi}. \quad (1.31)$$

The Bianchi identity for any abelian gauge field \mathcal{A} asserts that

$$d\mathcal{F} = 0. \quad (1.32)$$

So once again we get the Nielsen-Ninomiya theorem

$$0 = \int_{\mathcal{B}'} \frac{d\mathcal{F}}{2\pi} = \sum_\alpha \int_{S_\alpha} \frac{\mathcal{F}}{2\pi} = \sum_\alpha w(S_\alpha). \quad (1.33)$$

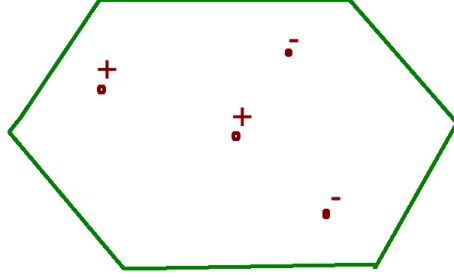


Figure 10: Generically, the band-crossing points in the Brillouin zone support Weyl fermions of positive and negative chirality. The Nielsen-Ninomiya theorem says that there are equally many of both types, as shown here.

So a more precise picture of the bad points in the Brillouin zone for a generic two-band system is as shown in fig. 10. A bad point labeled by + or - supports a gapless Weyl fermion of positive or negative chirality; the Nielsen-Ninomiya theorem says that there are equally many + and - points.

1.5 Some Examples

It is instructive to see concretely how two bad points of opposite chirality can annihilate as a parameter is varied. In relativistic physics, this can happen as follows (I am jumping ahead slightly, as we have not yet formulated the Nielsen-Ninomiya theorem for a system with more than two bands). Consider a four-band system in which the first two bands describe a Weyl fermion of positive chirality and the last two bands describe a Weyl fermion of negative chirality. Altogether, these four bands describe a four-component Dirac fermion. A Dirac fermion can have a bare mass, and when we add a bare mass term to the Hamiltonian, the band crossings disappear.

This is the usual relativistic picture, but in condensed matter physics, there is more freedom and the annihilation of two bad points can perfectly well occur for a two-band system. Consider the explicit Hamiltonian

$$H(p_1, p_2, p_3) = \begin{pmatrix} f(p_3) & p_1 - ip_2 \\ p_1 + ip_2 & -f(p_3) \end{pmatrix}. \quad (1.34)$$

If $f(p_3) = p_3$, this is the basic Hamiltonian $H = \vec{\sigma} \cdot \vec{p}$ of a Weyl fermion. More generally, if $f(p_3)$ is any smooth function with only simple zeroes, then a band crossing occurs at any zero of $f(p_3)$ (with $p_1 = p_2 = 0$), and gives a Weyl fermion of positive or negative chirality depending on the sign of df/dp_3 at the zero. A simple model with

$$f(p_3) = p_3^2 - a \quad (1.35)$$

gives, for $a > 0$, a pair of Weyl points with positive or negative chirality at $p_3 = \pm\sqrt{a}$. The two Weyl points coalesce for $a = 0$ and disappear for $a < 0$. This phenomenon does not arise

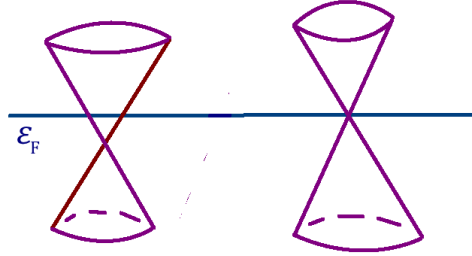


Figure 11: Band crossing below the fermi surface (left) or at the fermi surface (right).

in relativistic physics for a two-band system, since the effective Hamiltonian near $\vec{p} = a = 0$ does not have Lorentz symmetry or even rotation symmetry.

It is also of some interest to see how a band crossing point of multiplicity $s > 1$ can split into s points each of multiplicity 1. For this, consider the model Hamiltonian

$$H(p_1, p_2, p_3) = \begin{pmatrix} p_3 & \overline{g(x)} \\ g(x) & -p_3 \end{pmatrix}, \quad (1.36)$$

where g is a polynomial in the complex variable $x = p_1 + ip_2$. If $g(x) = x$, we have again the basic Weyl Hamiltonian. Band crossings occur at zeroes of g (with $p_3 = 0$). A simple zero gives a Weyl point of positive chirality and a multiple zero gives a band crossing point of higher multiplicity. So for example, the choice $g(x) = \prod_{i=1}^s (x - b_i)$ gives a model with a single band crossing point of multiplicity s if the b_i are all equal, and s such points each of multiplicity 1 if the b_i are generic.

1.6 Band Crossing At The Fermi Energy

So far, we have seen how band crossings modeled by a chiral Dirac Hamiltonian can arise naturally in condensed matter physics. But if we want this to have striking consequences, it will not do to have the band crossing at a random energy; we are really only interested in a band crossing that is at, or very near, the Fermi energy ε_F . Thus we want the picture to look like the one on the right and not the one on the left in fig. 11. Moreover, it will not do if the band structure is as shown on the right of the figure in part of the Brillouin zone, and like what is shown on the left in some other part. In that case, we will get a “normal metal” (because of the band crossing that is above or below ε_F), and its effects will probably swamp the more subtle “semi-metal” effects due to the band crossing which is at ε_F .

Ideally, we want the Fermi surface to consist only of a finite set of Weyl points at which two bands cross precisely at ε_F . There will have to be an even number of such points, with their chiralities adding to zero. How can we arrange that *all* band crossings occur at ε_F ? As a first step, how can we arrange so that they are all at the same energy? In the context of condensed matter physics, the way to do this is to find a material that has discrete spatial symmetries (and/or time-reversal symmetries) that permute all of the bad points. Some of

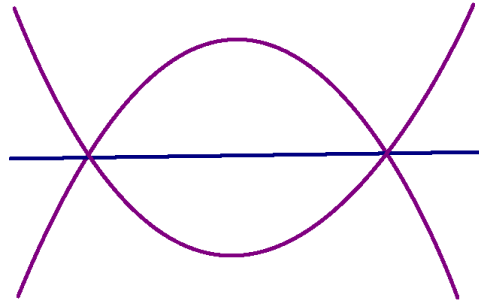


Figure 12: Two band-crossing points related by a discrete left-right symmetry. The fact that the number of electrons per unit cell is an integer makes it natural for both to occur at the fermi surface.

these symmetries have to be space or time orientation-reversing, since they have to exchange $+$ and $-$ points. The picture will then look more like what is shown in fig 12, with a left-right symmetry that exchanges the two bad points.

But how can we arrange so that the energy at which the band crossings occur is precisely ε_F ? Here we run into one of the beautiful things in this subject. We can get that for free, because the number of electrons per unit cell is an integer. For example, if there is precisely one electron per unit cell that is supposed to be filling the two bands in our model, the Fermi energy will be where we want it, because in fig. 12, at every value of the momentum \vec{p} away from the two bad points, precisely one state lies below ε_F and one lies above ε_F . Hence the band-crossing energy is the Fermi energy at half-filling. There are many important examples of this phenomenon. The oldest and best-known is graphene (in two dimensions), which we will discuss in Lecture Three. More recent examples involve Weyl semi-metals in three dimensions.

To be more exact, it is natural in this situation to have the band crossings at ε_F in the sense that, given a band Hamiltonian like the one we have assumed, any nearby band Hamiltonian with the same symmetries leads qualitatively to the picture of fig. 12. But this result is not forced by the universality class; a large enough deformation preserving the discrete symmetries will give an ordinary metal. We show in fig. 13 how to modify the band structure, preserving its symmetry, so that the level crossings are no longer at the Fermi energy.

1.7 Including Spin

On contemplating the statement “the band crossings will occur at ε_F if precisely one electron per unit cell is filling these two bands,” one may wonder if spin is being included in this counting. Actually, our discussion has been so general that it makes sense with or without spin. But there are two somewhat different cases.

In one case, spin-orbit couplings are important. It is not a good approximation to consider spin to be decoupled from orbital motion. The bands we have been drawing are the exact bands, taking spin and spin-dependent forces into account. In the second case, spin-dependent forces are small and to begin with one ignores them and considers orbital motion only. In such a case, the two bands described by a Dirac Hamiltonian are orbital bands. When we include spin, in first approximation we simply double the picture, so that now there are four bands –

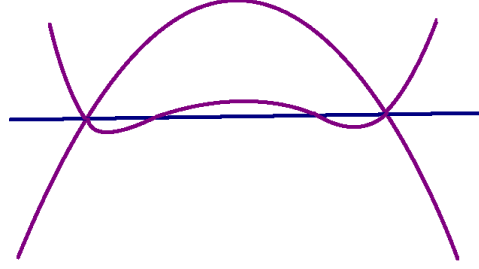


Figure 13: This band structure has the same left-right symmetry as in fig. 12, but describes an ordinary metal rather than a Weyl semimetal. That is because with this band structure, the energy of the band crossings – indicated by the horizontal line – passes below some of the states in the lower band and hence is below the fermi energy.

two copies of the familiar picture. In this approximation, we get 2 chiral Weyl fermions, and they have the same chirality because (if the spin is decoupled from orbital motion) the spin up and spin down electrons have the same band Hamiltonian and so the same chirality.

However, there always are spin-orbit forces in nature and generically the two pairs of bands will be split. The exact problem is a four-band problem. Assuming the density of electrons is such that 2 of the 4 bands are supposed to be filled, the crossings we care about (as they may be at or very near the Fermi energy) are those between the second and third bands, in order of increasing energy. The N band version of the Nielsen-Ninomiya theorem that we come to in a moment ensures that there will still be two Weyl crossings between the second and third bands (with the same chirality as before) but generically at slightly different energies and momenta. The Fermi energy cannot equal the energy of each of these crossings, and generically it does not equal either of them, but it will be close, assuming that the spin-orbit forces are weak.

A very crude picture of two nearby Weyl crossings neither of which is quite at the Fermi energy is in fig. 14. Naively this leads to a normal metal with a very small density of charge carriers, but this is not the full story because Fermi liquid theory does not work well when the density of charge carriers is very small.

1.8 A System With Many Bands

Now let us discuss the generalization of the Nielsen-Ninomiya theorem for an N band system. We assume that the density of electrons is such that k bands should be filled, for some integer $k < N$. We let \mathcal{H}_p be the full N -dimensional space of states at momentum p . At any value of p such that the k^{th} band (in order of increasing energy) does not meet the $k + 1^{\text{th}}$, \mathcal{H}_p has a well-defined subspace \mathcal{H}'_p spanned by the k lowest states. The definition of \mathcal{H}'_p does not make sense at points at which the k^{th} band meets the $k + 1^{\text{th}}$. Just as before, to make this happen we have to adjust three parameters, so as in fig. 5, there will be finitely many bad points in the Brillouin zone at which \mathcal{H}'_p is not defined.

Wherever \mathcal{H}'_p is well-defined, it defines a k -dimensional subspace of $\mathcal{H}_p \cong \mathbf{C}^N$. The space of all k -dimensional subspaces of \mathbf{C}^N is called the Grassmannian $\text{Gr}(k, N)$. If p_α is an isolated

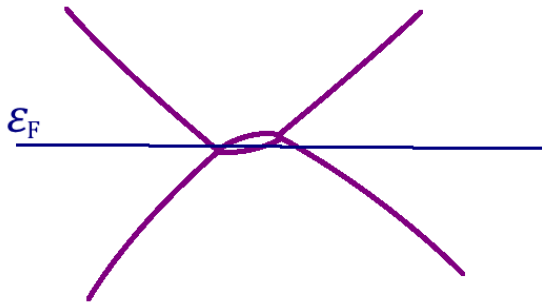


Figure 14: Two nearby band crossings that are not quite at the fermi energy.

point on which \mathcal{H}'_p is not defined, then \mathcal{H}'_p is defined on a small sphere S_α around p_α . Because $\pi_2(\text{Gr}(k, N)) \cong \mathbf{Z}$, we can attach an integer-valued winding number $w(S_\alpha)$ to each p_α .

Any of the explanations that we gave before for the case of two bands can be adapted to prove the Nielsen-Ninomiya theorem

$$\sum_{\alpha} w_{\alpha} = 0. \quad (1.37)$$

For example, let us consider the explanation based on the Berry connection. Letting \mathcal{B}' be as before the “good part” of the Brillouin zone with small neighborhoods of bad points removed, we have a rank k complex vector bundle $\mathcal{H}' \rightarrow \mathcal{B}'$ whose fiber at $p \in \mathcal{B}'$ is \mathcal{H}'_p . This is just the bundle spanned by the k lowest bands. On this bundle, there is a Berry connection, which is now a $U(k)$ gauge field.

It is defined as follows. To parallel transport $\psi_p \in \mathcal{H}'_p$ along a path $\gamma \subset \mathcal{B}'$ (fig. 8), we require that³

$$\langle \psi' | \frac{d}{ds} | \psi \rangle = 0, \quad \text{for all } \psi' \in \mathcal{H}'_p. \quad (1.38)$$

In other words, $d\psi/ds$ is required to be orthogonal to \mathcal{H}'_p , for all s . This gives a connection or $U(k)$ gauge field \mathcal{A} on $\mathcal{H}' \rightarrow \mathcal{B}'$. It has a curvature $\mathcal{F} = d\mathcal{A} + \mathcal{A} \wedge \mathcal{A}$. The winding number $w(S_\alpha)$ is

$$w(S_\alpha) = \int_{S_\alpha} c_1(\mathcal{H}') = \int_{S_\alpha} \frac{\text{Tr } \mathcal{F}}{2\pi}.$$

Using the Bianchi identity $d\text{Tr } \mathcal{F} = 0$, we get, with the help of Stokes’s theorem

$$0 = \int_{\mathcal{B}'} d \frac{\text{Tr } \mathcal{F}}{2\pi} = \sum_{\alpha} \int_{S_\alpha} \frac{\text{Tr } \mathcal{F}}{2\pi} = \sum_{\alpha} w(S_\alpha). \quad (1.39)$$

³The condition that $\psi_p(s)$ should be in $\mathcal{H}'_{p(s)}$ for all s determines the s dependence of $\psi_p(s)$ up to the freedom to add an s -dependent element of $\mathcal{H}'_{p(s)}$. This freedom is fixed by eqn. (1.38).

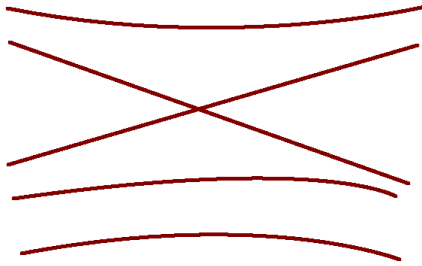


Figure 15: A generic crossing between the k^{th} band and the $k + 1^{\text{th}}$ band, for any k , is governed by the same chiral Dirac Hamiltonian that we originally encountered in the case of a two band system.

Thus, the proof using the Berry connection is the same as it was for two bands, except that we have to put a trace everywhere.

Generically, the winding number at a band point is ± 1 , just as in the two band case. The generic behavior at a crossing of winding number ± 1 is the familiar Weyl crossing between the k^{th} and $k + 1^{\text{th}}$ bands (fig. 15). So the points with winding number ± 1 give chiral Weyl fermions, and the Nielsen-Ninomiya theorem says that there are equally many of these of positive or negative chirality.

1.9 Two Dimensions

None of this relied on discrete symmetries, though much of it becomes richer if one does consider materials with discrete symmetries. But what if we want to get massless Dirac fermions in 2 space dimensions rather than 3? This will not work without discrete symmetries because generically there would be no band crossings as we vary the 2 parameters of a 2-dimensional Brillouin zone.

In $2 + 1$ dimensions, there are only three γ matrices $\gamma^0, \gamma^1, \gamma^2$, and they can be given a 2-dimensional representation. So a Dirac fermion in $2 + 1$ dimensions has only 2 components and the massless Dirac Hamiltonian is

$$H = \sigma_1 p_1 + \sigma_2 p_2. \tag{1.40}$$

(To derive this from the relativistic Dirac equation $\gamma^\mu \partial_\mu \psi = 0$, one basically follows the derivation of eqn. (1.15) in 3 space dimensions.) The energy levels are $\pm |p|$, and there is a level crossing at $p = 0$. We know that such a level crossing is nongeneric in 2 space dimensions, and concretely it is possible to perturb the Dirac Hamiltonian by adding a mass term:

$$H = \sigma_1 p_1 + \sigma_2 p_2 + \sigma_3 m. \tag{1.41}$$

The massive Dirac Hamiltonian has nondegenerate energy levels $\pm \sqrt{p^2 + m^2}$.

However, the mass term violates some symmetries. The *reflection* symmetry of $H = \sigma_1 p_1 + \sigma_2 p_2$ is

$$\mathbf{R}\psi(t, x_1, x_2) = \sigma_2 \psi(t, -x_1, x_2) \tag{1.42}$$

and the mass term

$$H' = m\sigma_3 \tag{1.43}$$

is odd under this. The mass term is similarly odd under time-reversal. With the Hamiltonian (1.41) and the standard representation⁴ of the σ -matrices, time-reversal is

$$\mathbb{T}\psi(t, \vec{x}) = \pm\sigma_1\psi(-t, \vec{x}). \tag{1.44}$$

The sign is actually physically meaningful and this turns out to be important in the theory of topological superconductors, though we will not explore that subject in the present lectures.

The physical reason that a mass term violates reflection symmetry \mathbb{R} and time-reversal symmetry \mathbb{T} is as follows. If ψ is a two-component electron field in two dimensions, then at any given value of the spatial momentum \vec{p} , one component of ψ is a creation operator and one is an annihilation operator. Hence ψ describes for each value of \vec{p} only a single state of charge 1 (along with a corresponding hole or antiparticle of charge -1). If the ψ particle is massive, we can study it in its rest frame and its one spin state will transform with spin $1/2$ or $-1/2$ under the rotation group. (In 2 space dimensions, the rotation group is just the abelian group $SO(2)$ and has 1-dimensional representations.) Either choice of sign is odd under \mathbb{R} or \mathbb{T} , so the mass term must violate those symmetries. By contrast, if $m = 0$, the fermion cannot be brought to rest, and in 2 space dimensions, we cannot define its spin.⁵ So the $m = 0$ theory can be \mathbb{R} - and \mathbb{T} -conserving.

This tells us that in a 2d crystal, it should be possible to find gapless Dirac-like modes as long as the crystal has a suitable \mathbb{R} or \mathbb{T} symmetry, and the gapless modes occur at an \mathbb{R} - or \mathbb{T} -invariant value of the momentum. It is not hard to give examples. The most famous example is graphene; we will discuss this case in Lecture Three. For now, I will just remark that rather as for Weyl points in 3 space dimensions, there are two versions, either a material that with spin included has an \mathbb{R} or \mathbb{T} symmetry that leads to a gapless mode, or a material with small spin-orbit forces that has the appropriate property if spin and spin-orbit forces are ignored. In the latter case, in the real world, one will get modes with a gap that is very small but not quite zero. This is indeed what happens in graphene [14].

⁴In studying a \mathbb{T} -invariant theory, it is often more convenient to start with real 2×2 gamma matrices γ_μ , and that is what we will generally do. In that case, the σ -matrices appearing in the Hamiltonian are the real matrices $\sigma_i = \gamma_0\gamma_i$, as in eqn. (1.17). With such a convention, \mathbb{T} acts by $\mathbb{T}\psi(t, \vec{x}) = \pm\gamma^0\psi(-t, \vec{x})$. Hidden in this statement is the following. Suppose that we expand the complex (Dirac) fermion field ψ in terms of two hermitian (Majorana) fermion fields χ_1, χ_2 , via $\psi = \chi_1 + i\chi_2$. Then χ_1 and χ_2 transform with opposite signs under \mathbb{T} : $\mathbb{T}\chi_1(t, \vec{x}) = \pm\gamma^0\chi_1(-t, \vec{x})$, $\mathbb{T}\chi_2(t, \vec{x}) = \mp\gamma^0\chi_2(-t, \vec{x})$. Since \mathbb{T} is antiunitary, $\mathbb{T}i = -i\mathbb{T}$, the opposite signs in the transformation of χ_1 and χ_2 ensures the simple transformation that we have claimed for ψ . Analogous statements hold later (footnote 7) when we describe the action of \mathbb{T} in 3 space dimensions.

⁵In D spacetime dimensions, the “spin” of a relativistic particle is always described by the transformation of the quantum state under the “little group,” the subgroup of the Lorentz group $SO(1, D - 1)$ that preserves its energy-momentum D -vector p^μ . For a massive particle, the little group is $SO(D - 1)$ and the spin is a representation of this group. For a massless particle, the little group is an extension of $SO(D - 2)$ by a noncompact group of “translations,” and the “spin” is actually determined by a representation of $SO(D - 2)$. (The “translation” part of the little group acts trivially in all conventional relativistic field theories. For an attempt to construct a theory in which this would not be the case, see [13].) For $D = 3$, $SO(D - 2)$ is trivial and there is no notion of the “spin” of a massless particle. In this explanation, we have ignored reflection and time-reversal symmetry. A massless particle in $D = 3$ does have a meaningful transformation under the discrete spacetime symmetries, when these are present.

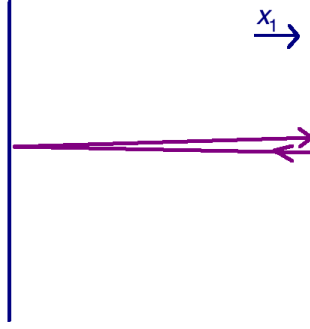


Figure 16: A particle reflecting at right angles from the boundary must reverse its helicity (the component of its angular momentum along the direction of motion) if it is to conserve its angular momentum.

1.10 Weyl Fermions And Fermi Arcs

Now we will begin our discussion of topologically-determined edge modes in condensed matter physics. We will do this in 3 space dimensions and we will start by considering a non-chiral massless Dirac fermion ψ . For now, never mind how to realize this in condensed matter physics. We suppose that ψ is confined to a half-space (possibly the interior of a crystal) and we ask what kind of boundary condition it should obey when it is reflected from a boundary. For reflection at right angles, as sketched in fig. 16, a simple boundary condition would conserve angular momentum.

By “conserving angular momentum,” I mean that for a boundary condition at $x_1 = 0$, the component J_1 of angular momentum around the x_1 axis should be conserved.⁶ Since the direction of motion is reversed in the scattering, the helicity has to be reversed. For a Dirac fermion, that is possible, because a Dirac fermion has both helicities. See eqn. (1.57) below for the angular momentum conserving but helicity-violating boundary condition that is possible for a Dirac fermion.

But what sort of boundary condition can we have for a massless Weyl fermion, which has only one helicity? Obviously, the boundary condition cannot reverse the helicity, and therefore it cannot conserve angular momentum. Any boundary condition will have to pick a preferred direction in the boundary plane. For a chiral Dirac Hamiltonian

$$H = -i\vec{\sigma} \cdot \frac{\partial}{\partial \vec{x}}, \tag{1.45}$$

a good boundary condition at $x_1 = 0$ is

$$M\psi|_{x_1=0} = \psi|_{x_1=0} \tag{1.46}$$

with

$$M = \sigma_2 \cos \alpha + \sigma_3 \sin \alpha \tag{1.47}$$

⁶In a crystal, J_1 might be conserved only mod n , for $n = 2, 3, 4$, or 6 . The argument below will show that the boundary condition on a Weyl fermion cannot conserve J_1 mod n for any $n > 1$.

for some angle α .

What makes this a good boundary condition is that it makes $H = -i\vec{\sigma} \cdot \vec{\nabla}$ hermitian. To prove that $H = -i\vec{\sigma} \cdot \vec{\nabla}$ is hermitian,

$$\langle \psi_1, H\psi_2 \rangle = \langle H\psi_1, \psi_2 \rangle, \quad (1.48)$$

one has to integrate by parts. A potential boundary term in this integration by parts vanishes because $\{M, \sigma_1\} = 0$, and our choice $M = \sigma_2 \cos \alpha + \sigma_3 \sin \alpha$ was made to ensure this. In particular, this will not work if we pick $M = \sigma_1$, and that again shows that the boundary condition cannot be invariant under rotation of the $x_2 - x_3$ plane. It cannot even preserve a nontrivial discrete subgroup of this rotation symmetry, such as might be present in a crystal.

Hermiticity would let us add additional momentum-dependent terms to the operator M that appears in the boundary condition, but in the low momentum limit, near the band-crossing point, it forces M to take the form that we have indicated, with some value of α . In continuum field theory, we could regard α as a free parameter. That is not really the situation in condensed matter physics. In a concrete model whose band structure in bulk leads to the existence of a band-crossing point described by a chiral Dirac Hamiltonian, solving the Schrodinger equation near the boundary of the system will determine an effective value of α . However, modifying the boundary, for example by adding an extra layer of atoms on the surface of a material, would generically change that value.

The value of α can be absorbed in a rotation of the $x_2 - x_3$ plane, so in analyzing the consequences of the boundary condition, we can consider the special case $\alpha = 0$, meaning that the boundary condition is $\sigma_2\psi| = \psi|$. Something very interesting happens when we solve the Schrodinger equation with this boundary condition. Let us try to solve the equation $H\psi = 0$ assuming that $\sigma_2\psi = \psi$ everywhere (not only on the boundary) and also assuming that $\partial\psi/\partial x_2 = 0$. Then

$$H\psi = -i(\sigma_1\partial_1 + \sigma_2\partial_2 + \sigma_3\partial_3)\psi = -i\sigma_1(\partial_1 - i\partial_3)\psi. \quad (1.49)$$

(Recall that $\sigma_3 = -i\sigma_1\sigma_2$, so $\sigma_3\psi = -i\sigma_1\psi$.) So we can solve $H\psi = 0$ with

$$\psi = \exp(ik_1x_3 + k_1x_1)\psi_0, \quad (1.50)$$

where ψ_0 is a constant spinor obeying

$$\sigma_2\psi_0 = \psi_0. \quad (1.51)$$

Moreover, this solution is plane-wave normalizable if

$$k_1 < 0. \quad (1.52)$$

More generally, for any real ε , we can solve $H\psi = \varepsilon\psi$ with

$$\psi = \exp(i\varepsilon x_2) \exp(ik_1x_3 + k_1x_1)\psi_0. \quad (1.53)$$

Assuming that our system is supported in the half-space $x_1 \geq 0$, with boundary at $x_1 = 0$, these solutions decay exponentially away from the boundary as long as $k_1 < 0$. They provide our first examples of topologically-determined edge-localized states in condensed matter physics.

For each energy ε that is close enough to the band-crossing energy so that the above analysis is applicable, we have found edge localized states that are supported on a ray $k_1 < 0$, $k_2 = \varepsilon$ in the $k_1 - k_2$ plane. At the endpoint $k_1 = 0$ of the ray, edge-localization breaks down and the solution becomes a plane wave (with momentum in the x_2 direction only). As such it is indistinguishable from a bulk state.

From the point of view of condensed matter physics, the fact that the edge-localized states of given energy lie on a straight line in momentum space is certainly not universal. We could add all sorts of higher order terms to the Hamiltonian and the boundary condition, and this would modify the dispersion relation of the edge-localized states, just as it would modify the dispersion relation for bulk states. However, the analysis that we have made is universal near the band-crossing point at $\vec{k} = 0$. This analysis shows that at any energy sufficiently near the band-crossing energy, there is an arc of edge-localized states, known as a Fermi arc [15].

An arc parametrizing edge-localized states can only end when the state in question ceases to be edge-localized. But at that point, as in our example, the edge-localized state becomes indistinguishable from some bulk plane wave state. In the presence of a boundary at $x_3 = 0$, the quantities k_1 , k_2 , and ε are conserved but k_3 is not. So the values of k_1 , k_2 , and ε at the endpoint of a Fermi arc will coincide with the corresponding values for some bulk plane wave state, with some value of k_3 . (In general, though not in our simple model, this value will depend on ε .)

A Fermi arc that has an end associated to a band-crossing point will inevitably have a second end, which will be associated to some other band-crossing point. Let us examine this matter from the point of view of the Nielsen-Ninomiya theorem. In general, we know that there are always multiple Weyl points in the Brillouin zone, say at momenta \vec{k}_α , $\alpha = 1, \dots, s$. In the presence of a boundary at $x_1 = 0$, the perpendicular part $k^\perp = k_1$ of the momentum is not conserved and we should classify the Weyl points only by $k^\parallel = (k_2, k_3)$.

In bulk, because momentum is conserved, gapless modes at different values of \vec{k} do not “mix” with each other and can be treated separately. But when we consider the behavior near a boundary, the “perpendicular” component k^\perp of the momentum is not conserved and we should only use k^\parallel . So we project the band points to 2 dimensions, as in fig. 17. As long as the projections k_α^\parallel of the Weyl points are all distinct, they will be connected pairwise by Fermi arcs.

But if two Weyl points of opposite chirality project to the same point in the boundary momentum space, as in fig. 18, then there is no need for either one to connect to a Fermi arc. From a low energy point of view, the two modes of opposite chirality combine to a Dirac fermion with both chiralities. A Dirac fermion admits a rotation-invariant boundary condition and can be gapped, as we discuss in section 1.11.

Of course, whether two given Weyl points coincide when projected to the boundary depends on which boundary face we consider. But the discrete symmetries that make Weyl points interesting can also make it natural, for some crystal facets, that two Weyl points have the same projection. In fact, this will have to happen if a crystal has a nontrivial group of rotations that preserves the plane $x_1 = 0$. Since a single Weyl fermion would not admit a boundary condition that preserves $J_1 \bmod n$ for any $n > 1$, in the presence of such a conservation law, we will never get just one Weyl fermion at a given value of k^\parallel .

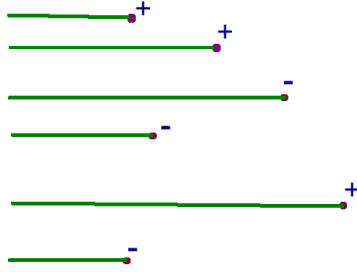


Figure 17: Projection of band-crossing points from the bulk Brillouin zone, which is parametrized by \vec{k} , to the surface Brillouin zone, which is parametrized by k^{\parallel} only. (In the picture, k^{\perp} runs horizontally and k^{\parallel} runs vertically.) Generically the band-crossing points occur at distinct values of k^{\parallel} . In this case, their projections are ends of Fermi arcs.

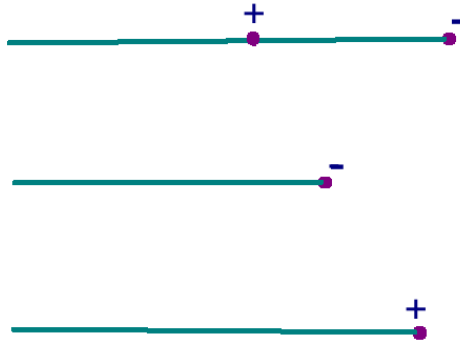


Figure 18: Discrete symmetries may make it natural for two or more band crossing points to occur at the same value of k^{\parallel} .

1.11 Gapless Boundary Modes From Dirac Fermions

It is also possible to get boundary-localized modes from Dirac fermions, and this is important in understanding topological insulators. In the absence of discrete symmetries, and without tuning any parameters, it is not natural in condensed matter physics to get a massless Dirac (as opposed to Weyl) fermion in three space dimensions. For a four-component fermion field ψ with both chiralities, mass terms are possible; in fact there are two such terms. The general Lorentz-invariant massive Dirac equation is

$$\left(\sum_{\mu} \gamma^{\mu} \partial_{\mu} - m - im' \gamma_5 \right) \psi = 0. \quad (1.54)$$

The corresponding Hamiltonian is

$$H = \gamma^0 \vec{\gamma} \cdot \vec{p} - im \gamma^0 - im' \gamma_1 \gamma_2 \gamma_3. \quad (1.55)$$

Relativistically, to get a massless Dirac fermion, we need a reason for $m = m' = 0$. Symmetries (spacetime or chiral symmetries) are the obvious place to look.

Let us consider the case of assuming time-reversal symmetry \mathbb{T} . This is enough to set one of the two parameters to 0 but not both. The Dirac equation becomes⁷

$$\left(\sum_{\mu} \gamma^{\mu} \partial_{\mu} - m \right) \psi = 0. \quad (1.56)$$

Generically m is not 0 but of course if we adjust one parameter, we can make m vanish.

In condensed matter physics, what we adjust to make a parameter in the Hamiltonian vanish might be, for example, the chemical composition of an alloy. However, we observe that while eqn. (1.55) is the general Lorentz-invariant Hamiltonian for this system, in condensed matter physics we should not assume Lorentz-invariance of the Hamiltonian and more terms are possible. The analysis of a more general Hamiltonian is more complicated. But there is a useful lesson that we can learn from a further study of the relativistic case.

Consider a Dirac fermion confined to the half-space $x_1 \geq 0$. The Dirac operator admits a natural, rotation-invariant boundary condition

$$\gamma_1 \psi|_{x_1=0} = \pm \psi|_{x_1=0}, \quad (1.57)$$

with some choice of sign. This stands in contrast to a Weyl fermion, which as we discussed earlier does not admit a rotation-symmetric boundary condition. The boundary condition (1.57) is helicity-violating, because γ_1 anticommutes with the chirality or helicity operator $\gamma_5 = i\gamma^0\gamma^1\gamma^2\gamma^3$. So it would not make sense for a Weyl fermion, which is an eigenstate of γ_5 and has only one helicity. Note that the boundary condition (1.57) is \mathbb{T} -conserving, with the action of \mathbb{T} defined in footnote 7, because γ_1 commutes with $\gamma^1\gamma^2\gamma^3$. The sign in the boundary condition can be reversed by $\psi \rightarrow \gamma_5\psi$, which also changes the sign of the mass parameter m in eqn. (1.56). So as long as we consider both signs of m , we can choose a + sign in the boundary condition.

⁷ This is invariant under $\mathbb{T}\psi(t, \vec{x}) = \gamma^1\gamma^2\gamma^3\psi(-t, \vec{x})$. We assume that the gamma matrices are real 4×4 matrices obeying $\{\gamma_{\mu}, \gamma_{\nu}\} = 2\eta_{\mu\nu}$, where $\eta_{\mu\nu} = \text{diag}(-1, 1, 1, 1)$.

Let x_{\parallel} be the coordinates along the boundary and

$$\gamma \cdot \partial^{\parallel} = \sum_{\mu \neq 1} \gamma^{\mu} \partial_{\mu} \quad (1.58)$$

the 2 + 1-dimensional Dirac operator along the boundary. We can obey the 3 + 1-dimensional Dirac equation in the half-space $x_1 \geq 0$ with

$$\psi = \exp(mx_1)\psi_{\parallel}(x_{\parallel}) \quad (1.59)$$

where

$$\gamma_1 \psi_{\parallel} = \psi_{\parallel}, \quad \gamma \cdot \partial^{\parallel} \psi_{\parallel}(x_{\parallel}) = 0. \quad (1.60)$$

For $m > 0$, this solution is highly unnormalizable. But for $m < 0$, it is plane-wave normalizable and localized along the boundary.

To be more precise, since ψ_{\parallel} was constrained to obey the massless 2 + 1-dimensional Dirac equation

$$\gamma \cdot \partial^{\parallel} \psi_{\parallel}(x_{\parallel}) = 0, \quad (1.61)$$

we get a 2 + 1-dimensional massless Dirac fermion. (This is a standard 2-component Dirac fermion in 2 + 1 dimensions, because half of the components of the original 4-component 3 + 1-dimensional Dirac fermion are removed by the constraint $\gamma_1 \psi_{\parallel} = \psi_{\parallel}$.)

In a T-invariant theory, a phase that is gapped in bulk and has a single boundary-localized massless Dirac fermion is essentially different from a phase that is gapped both on the bulk and on the boundary. That is because once we find a single boundary-localized massless fermion, small T-invariant perturbations, even if they violate Lorentz symmetry, will not cause the boundary to be gapped. Indeed, we recall that T-invariance does not allow a single 2 + 1-dimensional Dirac fermion to acquire a mass.

However, T-invariance would permit a *pair* of Dirac fermions in 2 + 1 dimensions to acquire bare masses. The T-invariant Dirac equation for such a pair is⁸

$$\left(\sum_{\mu=0}^2 \gamma^{\mu} \partial_{\mu} - i \begin{pmatrix} 0 & m \\ -m & 0 \end{pmatrix} \right) \begin{pmatrix} \psi_1 \\ \psi_2 \end{pmatrix} = 0. \quad (1.62)$$

(Upon diagonalizing the mass term, one learns that this gives two 2 + 1-dimensional massive Dirac fermions with equal and opposite masses.) Thus, in a condensed matter system of 3 space dimensions with T-invariance and no other special properties, the number of boundary-localized Dirac fermions will be generically either 0 or 1. These are two different phases; one cannot pass between them, maintaining T-invariance, as long as the bulk theory is gapped. (When the bulk is gapless, a boundary gapless mode can disappear by becoming indistinguishable from a bulk mode.) The case that there is a gapless Dirac mode on the boundary is the 3-dimensional topological insulator [16]. Topological band theory gives a powerful way to understand this phase, but we will not explore that here.

What we have said shows that when the mass of a bulk Dirac fermion passes through 0, this results in a phase transition between an ordinary insulator and a topological insulator. That is a

⁸T acts by $T\psi_i(t, \vec{x}) = \gamma^0 \psi_i(-t, \vec{x})$, $i = 1, 2$. The mass term has been chosen to be hermitian while ensuring T-invariance.

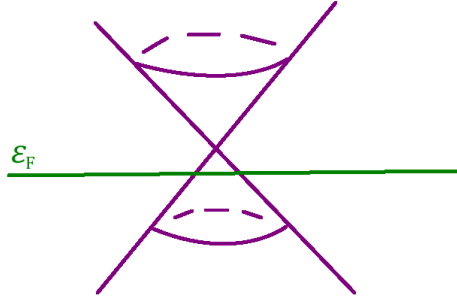


Figure 19: Generically, the band crossing point of the edge-localized mode of a topological insulator in 3 space dimensions does not occur at the Fermi energy. Accordingly, the boundary has much in common with a normal metal.

particularly simple path between these two phases that looks natural from a relativistic point of view. But this path is nongeneric in the context of condensed matter physics, provided \mathbb{T} is the only pertinent symmetry, because in condensed matter physics the Hamiltonian will generically contain additional terms that do not respect Lorentz invariance. It turns out [17, 18] that generically the transition from an ordinary insulator to a topological one is a more complicated process with an intermediate conducting phase.⁹ With \mathbb{P} assumed as well as \mathbb{T} , the simple model in which the phase transition between the two types of insulator involves a massless Dirac fermion is indeed valid. We return to this point at the end of section 1.12.

Generically, in the context of condensed matter physics, the fermi energy ε_F of a topological insulator does not pass through the Dirac point in the boundary theory. So (fig. 19) the boundary of a topological insulator is more like an ordinary metal than the Weyl semimetals that we talked about before. Relativistically, the boundary theory is analogous to the theory of a massless Dirac fermion with a nonzero chemical potential.

1.12 Discrete Lattice Symmetries and Massless Dirac Fermions

Because the Hamiltonian need not be Lorentz-invariant, we have really not yet found a way to generate massless Dirac fermions in condensed matter physics, even assuming time-reversal symmetry and varying one parameter. However, massless Dirac fermions can become natural if more symmetry is assumed. In what follows, we sketch a construction in [19], leaving some details to the reader. For some of the background, see [20].

First, let us reconsider the relativistic massless Dirac fermion in $3 + 1$ dimensions. The Hamiltonian is $H = \gamma_0 \vec{\gamma} \cdot \vec{p}$, where now the γ^μ are 4×4 matrices and we assume no chiral projection. Equivalently, the Hamiltonian is conjugate to

$$H = \begin{pmatrix} \vec{\sigma} \cdot \vec{p} & 0 \\ 0 & -\vec{\sigma} \cdot \vec{p} \end{pmatrix}. \quad (1.63)$$

⁹ Starting with a trivial insulator, as one varies a parameter, the system undergoes a transition described in section 1.5, with appearance of a pair of Weyl points of opposite chirality. This happens simultaneously at two equal and opposite values of \vec{p} , exchanged by \mathbb{T} . Going further, the Weyl points reconnect and annihilate, leaving a topological insulator.

The energy levels are $\pm|\vec{p}|$, each occurring with multiplicity 2.

One explanation of the twofold degeneracy of the bands is the following. The massless nonchiral Dirac Hamiltonian has both time-reversal symmetry T and parity symmetry P . Each of these reverses the sign of the spatial momentum, so the product PT is a symmetry at any given momentum. But PT is an antiunitary symmetry, and in acting on a fermion state, $(\mathsf{PT})^2 = -1$. The existence of an antiunitary symmetry that leaves \vec{p} fixed and squares to -1 means that the energy levels at each momentum have a Kramers degeneracy, which accounts for the doubling.

It is perfectly natural in condensed matter physics to consider a material with PT symmetry. Indeed, many nonmagnetic materials have T symmetry, and many crystals have P symmetry (usually called inversion symmetry in the context of condensed matter). In a PT -symmetric material, all bands will have 2-fold degeneracy. If spin-orbit forces can be ignored, this is simply the 2-fold degeneracy resulting from spin. However, PT symmetry forces an exact 2-fold degeneracy of all bands even with spin-dependent forces included.

The question arises of whether in a PT -symmetric material, and for the moment assuming no further symmetry, the generic 2-fold degeneracy of the bands becomes a 4-fold degeneracy somewhere in the Brillouin zone. To answer this question, we consider a generic PT symmetric system with 4 bands. The unitary group acting on 4 states (that is, on the states of 4 bands at a given value of \vec{p}) is in general $U(4)$. The subgroup of this group that commutes with an antiunitary symmetry PT that satisfies $(\mathsf{PT})^2 = -1$ is $Sp(4)$. The fifteen 4×4 traceless hermitian matrices that might conceivably lift the band degeneracy transform under $Sp(4)$ as $\mathbf{15} = \mathbf{5} \oplus \mathbf{10}$. The PT -invariant ones transform as $\mathbf{5}$. In fact, the group $Sp(4)$ is the double cover $\text{Spin}(5)$ of $SO(5)$, and the $\mathbf{5}$ of $Sp(4)$ is just the defining 5-dimensional representation of $SO(5)$.

For a basis of 5 traceless, hermitian, PT -invariant 4×4 matrices, we can take gamma matrices¹⁰ $\hat{\gamma}_1, \dots, \hat{\gamma}_5$, obeying $\{\hat{\gamma}_i, \hat{\gamma}_j\} = 2\delta_{ij}$. The general PT -invariant traceless 4-band Hamiltonian is therefore

$$H = \sum_{i=1}^5 A_i(\vec{p}) \hat{\gamma}_i. \quad (1.64)$$

To get a 4-fold band degeneracy, we need to make the five functions $A_i(\vec{p})$ simultaneously vanish. Generically, in spatial dimension 3, this will not happen anywhere in the Brillouin zone. Therefore, to get a massless Dirac fermion, we need to assume more symmetry.

Let us consider a crystal with a \mathbf{Z}_n rotation symmetry, where the most convenient values¹¹ of n are 4 and 6. We assume that the band degeneracy of interest will occur at a \mathbf{Z}_n -invariant value of the momentum. (In general, only the subgroup of \mathbf{Z}_n that leaves fixed the momentum at which a given band degeneracy occurs will be relevant in protecting that degeneracy.) We can arrange the crystal axes so that \mathbf{Z}_n leaves p_1 fixed. We can also assume, without essential loss of generality, that the \mathbf{Z}_n -invariant value of the momentum at which there will be a massless fermion satisfies $p_2 = p_3 = 0$. Further, we can assume that near $p_2 = p_3 = 0$, \mathbf{Z}_n is generated by an element R that acts as a $2\pi/n$ rotation of the $p_2 - p_3$ plane, leaving p_1 fixed.

R will be realized on the 4 fermion bands as an element of $Sp(4)$; it will act on the 5 gamma

¹⁰We place hats on these gamma matrices as they do not coincide with the $SO(3,1)$ gamma matrices that were used in the relativistic description. We explain the relationship in eqn. (1.67).

¹¹A similar story holds for $n = 3$ with slight modifications.

matrices as an element of $SO(5)$. A general element of $SO(5)$ of order n has eigenvalues $1, \exp(\pm 2\pi i r/n), \exp(\pm 2\pi i s/n)$ in the **5** representation, for some integers r, s which we can take to be nonnegative and ¹² $\leq n$. For a reason that we will explain in a moment, we can assume that $r + s$ is odd. Different cases are of interest for condensed matter physics, but to get a massless Dirac fermion we need r (or s) to equal 1 while the other is nonzero. Since $r + s$ is odd, if $r = 1$ and $s \neq 0$ then s is even and ≥ 2 .

The reason that $r + s$ should be odd is as follows. If the gamma matrices transform under R as $1, \exp(\pm 2\pi i r/n), \exp(\pm 2\pi i s/n)$, then the 4 bands that they act on transform under R as $\exp(\pi i(\pm r \pm s)/n)$. But on fermions one wants $R^n = -1$, which corresponds to $r + s$ odd. For $r = 1$, the eigenvalues of R acting on the 4 bands are

$$\exp(\pm \pi i/n) \exp(\pm 2\pi i s'/n), \quad s' = s/2, \quad (1.65)$$

where s' is an integer since s is even.

We can pick a basis of the 5 gamma matrices so that $\hat{\gamma}_1$ is R -invariant, the $\hat{\gamma}_2 - \hat{\gamma}_3$ plane is rotated by R by an angle $2\pi/n$, and the $\hat{\gamma}_4 - \hat{\gamma}_5$ plane is rotated by R by an angle $2\pi s/n$. Let us now analyze the Hamiltonian, first along the axis $p_2 = p_3 = 0$, and then slightly away from this axis.

At $p_2 = p_3 = 0$, the momentum is R -invariant. The only R -invariant gamma matrix is $\hat{\gamma}_1$, so a general R -invariant Hamiltonian is $H = \hat{\gamma}_1 A(p_1)$. It is natural for $A(p_1)$ to have a simple zero at some value of p_1 , and that is where a massless Dirac fermion will occur. Expanding the Hamiltonian in powers of p_2 and p_3 , because of the assumption that $r = 1$, the $\hat{\gamma}_2 - \hat{\gamma}_3$ plane is rotated by R just like the $p_2 - p_3$ plane and the Hamiltonian can have a term $B(p_1)(\hat{\gamma}_2 p_2 + \hat{\gamma}_3 p_3)$. The coefficients of $\hat{\gamma}_4, \hat{\gamma}_5$ vanish up to higher order in p_2, p_3 because $s \geq 2$. Thus to linear order in p_2, p_3 , the Hamiltonian is

$$H = A(p_1)\hat{\gamma}_1 + B(p_1)(\hat{\gamma}_2 p_2 + \hat{\gamma}_3 p_3). \quad (1.66)$$

There is a massless Dirac fermion at any simple zero of $A(p_1)$, assuming that $B(p_1) \neq 0$ at that point.

The assumption that r (or s) equals 1 is actually rather natural, for the following reason. It led to the result (1.65) for the transformation of the 4 bands under R . But this is the result that one would expect if the 4 bands of interest are the tensor product of 2 spatial bands with 2 spin states. The eigenvalues of a $2\pi/n$ rotation acting on the spin states of a spin 1/2 particle are $\exp(\pm \pi i/n)$, and the eigenvalues of such a rotation acting on 2 spatial bands in a PT-invariant system will be $\exp(\pm 2\pi i s'/n)$ for some integer s' .

From a relativistic point of view, one would account for what we have found by saying that what microscopically is the spatial rotation R has behaved in the effective theory at low energies as a combination of a spatial rotation and a chiral symmetry. The chiral symmetry, which is expressed in the above analysis as the rotation of the $\hat{\gamma}_4 - \hat{\gamma}_5$ plane, arises if $s \neq 0$. To explain this point more fully, observe that the relation between the five terms in the PT-invariant relativistic Dirac Hamiltonian (1.55) and the five terms in eqn. (1.64) comes from

$$\gamma_0 \gamma_i = \hat{\gamma}_i \quad (i = 1, 2, 3), \quad -i\gamma^0 = \hat{\gamma}_4, \quad i\gamma_1 \gamma_2 \gamma_3 = \hat{\gamma}_5. \quad (1.67)$$

¹²We can further restrict to $r \leq n/2$. We could restrict r, s to be both $\leq n/2$, but then we would need to include a possible overall minus sign in eqn. (1.65) below, because of the fact that the group $Sp(4)$ that acts on the bands is a double cover of the group $SO(5)$ that acts on the gamma matrices.

Thus the rotation of the $\hat{\gamma}^4 - \hat{\gamma}^5$ plane is a rotation of the parameters m and m' in the relativistic Hamiltonian (1.55). In relativistic physics, a symmetry that rotates those parameters is usually called a chiral symmetry and such a symmetry forces the vanishing of the fermion mass.

In the preceding analysis, we have made use only of PT and not of separate P and T symmetry. This is appropriate if a material has only PT symmetry and not separate P and T symmetries, or if the material has both symmetries but the band degeneracy of interest occurs at a value of the momentum that is PT-invariant but not P- or T-invariant. A further interesting construction [21] becomes possible in a material that does have separate P and T symmetry, and governs band degeneracies that occur at values of the momentum that are invariant under both symmetries. It turns out to be necessary to consider non-symmorphic symmetries (symmetries that mix rotations and partial lattice translations in an essential way). For an introduction, focusing on an analogous problem in 2 space dimensions, see [22].

As a simple example of the consequences of assuming both P and T symmetry, we reconsider the transition, discussed in section 1.11, between an ordinary insulator and a topological one. In fact, with both P and T symmetry,¹³ this phase transition occurs when a Dirac fermion mass passes through 0, rather than by the more complicated route described in footnote 9. The point is that PT symmetry enables us to express the Hamiltonian in terms of five functions, as in eqn. (1.64) (with eqn. (1.67) as a recipe to express the relativistic Hamiltonian (1.55) in terms of the five functions A_i of eqn. (1.64)). When we assume separate T and P symmetry, only one¹⁴ of the five functions A_i , namely $A_4 = m$, is T- and P-invariant. The other A_i are all odd and vanish at the T- and P-invariant point $\vec{p} = 0$. So at $\vec{p} = 0$, a 4-fold band degeneracy can be achieved by setting to 0 the one parameter m .

1.13 Simple Examples Of Band Hamiltonians

We conclude by giving simple examples of band Hamiltonians to illustrate some of these ideas.

One goal is to describe a simple band Hamiltonian that can be approximated near $\vec{p} = 0$ by the chiral Dirac Hamiltonian $H = \vec{\sigma} \cdot \vec{p}$. For this purpose, the main difference between band theory and the relativistic problem is that in band theory the components of the momentum are periodic variables. We assume a simple cubic lattice of lattice spacing a so that the linear components of the momentum have period $2\pi/a$. To write a band Hamiltonian, we can replace the linear component p_i , $i = 1, 2, 3$ of the electron momentum by $\frac{1}{a} \sin(p_i a)$, which has the correct periodicity and is equivalent to p_i for small p_i . This motivates the band Hamiltonian

$$H = \frac{1}{a} \sum_{i=1}^3 \sigma_i \sin(p_i a). \quad (1.68)$$

The formula $\sin u = (e^{iu} - e^{-iu})/2i$ shows that, when written in coordinate space, this Hamiltonian describes nearest neighbor hopping on the cubic lattice.

¹³We assume that the bands are not all even or all odd under P, so that $P \neq \pm 1$ as an element of $Sp(4)$. Otherwise the low energy physics is quite different.

¹⁴A simple way to see this is to observe that P must be an element of $Sp(4)$ obeying $P^2 = 1$, $P \neq \pm 1$. Any such element (other than $P = \pm 1$) acts on the gamma matrices as $\text{diag}(-1, -1, -1, -1, 1)$ (up to conjugation) and so leaves invariant precisely one linear combination of the A_i . With standard relativistic conventions that were used in writing eqn. (1.55), P acts by $P\psi(t, \vec{x}) = i\gamma^0\psi(t, -\vec{x})$ and the P-invariant coupling is $A_4 = m$.

For $\vec{p} \rightarrow 0$, this Hamiltonian can be approximated by $\vec{\sigma} \cdot \vec{p}$, so there is a Weyl point of positive chirality at $\vec{p} = 0$. However, a little reflection shows that the model actually has a total of 8 Weyl points in the Brillouin zone; they are the 8 points at which each of the p_i equals 0 or π/a . Using the criterion (1.21), the reader can verify that 4 of these Weyl points have positive chirality and 4 have negative chirality. Thus the net chirality is 0, in keeping with the Nielsen-Ninomiya theorem. Indeed, the Nielsen-Ninomiya theorem was inspired by examples such as this one.

We can similarly write a periodic version of the non-chiral 4-component Dirac Hamiltonian (1.55):

$$H = \frac{1}{a} \sum_{i=1}^3 \gamma_0 \gamma_i \sin(p_i a) - im\gamma^0. \quad (1.69)$$

We have set $m' = 0$ to ensure \mathbb{T} and \mathbb{P} invariance (assuming that m is an even function of \vec{p}). If $m = 0$, there are massless Dirac fermions at the same 8 points as before. If m is nonzero, the system is gapped for all \vec{p} . It is an insulator and in fact a trivial one if m is a constant. However, we get something new if m is a more general periodic function of \vec{p} . Assuming that m is small, the term in H proportional to m is only important near the 8 points that support an almost massless Dirac fermion. Moreover, all that really matters is the sign of m at those 8 points. We would like $m(\vec{p})$ to have a finite Fourier expansion in powers of $\exp(\pm ip_i a)$ (so that the position space Hamiltonian has finite range). Even with this constraint, there is no problem to vary independently the sign of $m(\vec{p})$ at the 8 points of interest. When one of those signs passes through 0, an edge-localized massless Dirac fermion appears or disappears. Thus this Hamiltonian with a suitable function $m(\vec{p})$ gives a simple model of a topological insulator in 3 space dimensions.

What we have described is somewhat analogous to the Haldane model [23] of a topologically non-trivial band insulator in 2 space dimensions. We will come to that model in section 3.3.

2 Lecture Two

2.1 Chern-Simons Effective Action

Today we will begin with an introduction to some aspects of the integer quantum Hall effect. First I just want to explain from the point of view of effective field theory why there is an integer quantum Hall effect in the first place. We consider a material that not only is an insulator, but more than that has no relevant degrees of freedom – not even topological ones – in the sense that its interaction with an electromagnetic field can be described by an effective action for the $U(1)$ gauge field A of electromagnetism only, without any additional degrees of freedom. (This would certainly not be true in a conductor, whose interaction with an electromagnetic field cannot be described without including the charge carriers in the description, along with A . But more subtly, as we will discuss, it is not true in a fractional quantum Hall system, whose effective field theory requires topological degrees of freedom coupled to A .)

In a 3 + 1-dimensional material with no relevant degrees of freedom, the effective action for the electromagnetic field can have all sorts of terms associated to various familiar effects. For example, ferromagnetism and ferroelectricity correspond to terms in the effective action that

are linear in \vec{E} or \vec{B}

$$I' = \int_{W_3 \times \mathbf{R}} (\vec{a} \cdot \vec{E} + \vec{b} \cdot \vec{B}). \quad (2.1)$$

(Here W_3 is the spatial volume of the material and \mathbf{R} parametrizes the time, so the “world-volume” of the material is $M_4 = W_3 \times \mathbf{R}$.) Similarly, electric and magnetic susceptibilities correspond to terms bilinear in \vec{E} or \vec{B} :

$$I'' = \int_{W_3 \times \mathbf{R}} (\alpha_{ij} E_i E_j + \beta_{ij} B_i B_j). \quad (2.2)$$

And so on.

All these terms are manifestly gauge-invariant in the sense that they are integrals of gauge-invariant functions: the integrands are constructed only from \vec{E} and \vec{B} (and possibly their derivatives). In 2 + 1 dimensions, there is a unique term that is gauge-invariant but does *not* have this property. This is the Chern-Simons coupling

$$\text{CS} = \frac{1}{4\pi} \int_{M_2 \times \mathbf{R}} d^3x \epsilon^{ijk} A_i \partial_j A_k. \quad (2.3)$$

The density $\epsilon^{ijk} A_i \partial_j A_k$ that is being integrated is definitely not gauge-invariant, but the integral is gauge-invariant up to a total derivative. In fact, under $A_i \rightarrow A_i + \partial_i \phi$, we have

$$\epsilon^{ijk} A_i \partial_j A_k \rightarrow \epsilon^{ijk} A_i \partial_j A_k + \partial_i (\epsilon^{ijk} \phi \partial_j A_k). \quad (2.4)$$

Roughly speaking, this shows that CS is gauge-invariant, but we have to be more careful because of electric charge quantization. If the quantum of electric charge is carried by a field ψ of charge 1 transforming as

$$\psi \rightarrow e^{i\phi} \psi, \quad (2.5)$$

then we should consider ϕ to be defined only modulo 2π :

$$\phi \cong \phi + 2\pi. \quad (2.6)$$

Given this fact, the previous proof of gauge-invariance of CS, in which ϕ was assumed to be single-valued, is not quite correct. We will be more careful in a moment.

Before I go on, though, I want to point out that logically, one could consider a theory in which one is only allowed to make a gauge transformation $A_i \rightarrow A_i + \partial_i \phi$ with a single-valued ϕ . But that theory is not the real world. Dirac showed that the Schrodinger equation of electrons, protons, and neutrons can be consistently coupled with magnetic monopoles, and that this consistency is only possible because the Schrodinger equation is invariant under gauge transformations in which $e^{i\phi}$ is single-valued although ϕ is not. This is needed to make the Dirac string unobservable (fig. 20).

Anyway our microscopic knowledge that the Schrodinger equation is invariant under any gauge transformation such that $e^{i\phi}$ is single-valued (even if ϕ is not single-valued) implies constraints on the effective action that we would not have without that knowledge. We want to understand those constraints.



Figure 20: The Dirac string emanating from a magnetic monopole is unobservable because the laws of nature are invariant under gauge transformations in which $e^{i\phi}$ is single-valued, but ϕ is not.

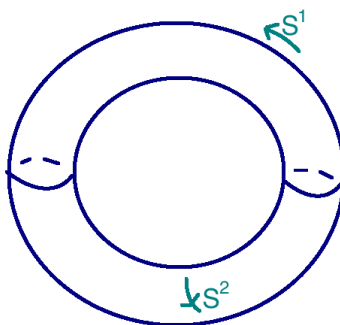


Figure 21: A 2 + 1-dimensional manifold $S^2 \times S^1$ that is used in analyzing the gauge-invariance of the Chern-Simons action.

2.2 Quantization Of The Chern-Simons Coupling

To do this, we will consider the following situation: we take our two-dimensional material to be a closed two-manifold, for instance S^2 , and we will take “time” to be a circle S^1 of circumference β . (For example, we might be computing $\text{Tr} e^{-\beta H}$.) Thus we consider a material whose “worldvolume” is $M_3 = S^2 \times S^1$ (fig. 21).

One might not be able to engineer this situation in the real world, but it is clear that the Schrodinger equation makes sense in this situation. So we can consider it in deducing constraints on the effective action that can arise from the Schrodinger equation.

The gauge field that we want to consider on $M_3 = S^2 \times S^1$ is as follows. We place a unit of Dirac magnetic flux on S^2 :

$$\int_{S^2} dx_1 dx_2 \frac{F}{2\pi} = 1. \quad (2.7)$$

(This is the right quantum of flux if the covariant derivative of the electron is $D_i \psi = (\partial_i - iA_i)\psi$, meaning that I am writing A for what is often called eA . This lets us avoid factors of e in many formulas.)

And we take a constant gauge field in the S^1 or time direction:

$$A_0 = \frac{s}{\beta}, \quad (2.8)$$

with constant s . For this gauge field, one can calculate¹⁵

$$\text{CS} = \frac{1}{4\pi} \int_{M_3=S^2 \times S^1} d^3x \epsilon^{ijk} A_i \partial_j A_k = s. \quad (2.9)$$

Note that the holonomy of A around the “time” circle is

$$\exp\left(i \int_0^\beta A_0 dt\right) = \exp\left(i \int_0^\beta (s/\beta) dt\right) = \exp(is). \quad (2.10)$$

The gauge transformation

$$\phi = \frac{2\pi t}{\beta}, \quad (2.11)$$

which was chosen to make $e^{i\phi}$ periodic, acts by

$$s \rightarrow s + 2\pi \quad (2.12)$$

and so leaves the holonomy invariant. (This must be true, because with my normalization of A , this holonomy is the phase factor when an electron is parallel-transported around the circle and so is physically meaningful.)

So we have in this example $\text{CS} = s$, and a gauge transformation can act by $s \rightarrow s + 2\pi$. Thus CS is not quite gauge-invariant; it is only gauge-invariant mod 2π . Here we must remember what is essentially the same fact that was exploited by Dirac in his theory of the magnetic monopole. The classical action I enters quantum mechanics only via a factor $\exp(iI)$ in the Feynman path integral (or $\exp(iI/\hbar)$ if one restores \hbar), so it is enough if I is well-defined and gauge-invariant mod $2\pi\mathbf{Z}$. Since CS is actually gauge-invariant mod $2\pi\mathbf{Z}$ (we showed this in an example but it is actually true in general), it can appear in the effective action with an integer coefficient:

$$I_{\text{eff}} = k\text{CS} + \dots$$

2.3 Quantization Of The Hall Conductivity

The point of this explanation has been to explain why k has to be an integer – sometimes called the “level.” The fact that k is an integer gives a macroscopic explanation of the quantization of the Hall current. Indeed for any material whose interaction with an electromagnetic potential A is governed by an effective action I_{eff} , the induced current in the material is

$$J_i = -\frac{\delta I_{\text{eff}}}{\delta A_i}. \quad (2.13)$$

¹⁵This is actually a slightly tricky calculation, because in the presence of nonvanishing magnetic flux on S^2 , the gauge field A_i has a Dirac string singularity. A safe way to do the calculation is to compute the derivative of CS with respect to s , using the fact that in any infinitesimal variation of A , one has $\delta\text{CS} = (1/4\pi) \int \epsilon_{ijk} \delta A_i F_{jk}$, which is written only in terms of gauge-invariant quantities F_{jk} and δA_i . Evaluating this formula for the case that $\delta A_i = \partial A_i / \partial s = \delta_{i0}$ and that there is one unit of magnetic flux on S^2 , one finds that $\partial\text{CS}/\partial s = 1$. Using also the fact that CS vanishes at $s = 0$, one arrives at eqn. (2.9).

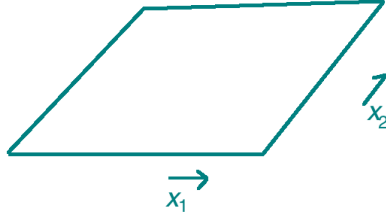


Figure 22: A two-dimensional sample.

We are interested in the case that

$$I_{\text{eff}} = k\text{CS} = \frac{k}{4\pi} \int_{M_3} d^3x \epsilon^{ijk} A_i \partial_j A_k. \quad (2.14)$$

Let us consider a material sitting at rest at $x_3 = 0$ and thus parametrized by x_1, x_2 (fig. 22). The current in the x_2 direction is

$$J_2 = -\frac{\delta I_{\text{eff}}}{\delta A_1} = \frac{kF_{01}}{2\pi} = \frac{kE_1}{2\pi}. \quad (2.15)$$

This is called a Hall current: an electric field in the x_1 direction has produced a current in the x_2 direction. The Hall current has a quantized coefficient $k/2\pi$ (usually called ke^2/h ; recall that my A is usually called eA and that I set $\hbar = 1$ so $h = 2\pi$), where the quantization follows from the fact that CS is not quite gauge-invariant.

One may wonder “How then can one have a fractional quantum Hall effect?” I will give a short answer for now, postponing more detail for Lecture Three.¹⁶ One cannot get an integer quantum Hall effect in a description in which A is the only relevant degree of freedom. However, from a macroscopic point of view, this can happen in a material that generates an additional “emergent” $U(1)$ gauge field a that only propagates in the material. We normalize a so that it has the same flux quantum¹⁷ 2π as A . We will write $f_{ij} = \partial_i a_j - \partial_j a_i$ for the field strength of a . An example of a gauge-invariant effective action that leads to a fractional quantum Hall effect is

$$I_{\text{eff}} = \frac{1}{2\pi} \int_{M_3} d^3x \epsilon^{ijk} A_i \partial_j a_k - \frac{r}{4\pi} \int_{M_3} d^3x \epsilon^{ijk} a_i \partial_j a_k. \quad (2.16)$$

¹⁶For a useful introduction to the very rich subject of effective field theories of the fractional quantum Hall effect, with references to the literature up to that time, see [24].

¹⁷In the context of condensed matter physics, it is unphysical to assume that an emergent gauge field a gauges a noncompact gauge group \mathbf{R} rather than the compact gauge group $U(1)$. In that case, there would be an exactly conserved current $\mathbf{j}_i = \frac{1}{2}\epsilon_{ijk} f^{jk}$ and correspondingly, the space integral $\mathbf{q} = \int d^2x \mathbf{j}^0 = \int d^2x f_{12}$ would be an exactly conserved quantity. There is no exactly conserved quantity in condensed matter physics that is a candidate for \mathbf{q} . If the emergent gauge group is $U(1)$ rather than \mathbf{R} , then “monopole operators” can be added to the Hamiltonian, breaking the conservation of \mathbf{q} . Because the emergent gauge group is $U(1)$, there is a nontrivial Dirac flux quantum, and we normalize a so that this quantum is 2π . Accordingly, the parameter r in eqn. (2.16) must be an integer.

An oversimplified explanation of why this gives a fractional quantum Hall effect is the following. One argues that as a appears only quadratically in the effective action, one can integrate it out using its equation of motion. This equation is

$$f = \frac{1}{r}F, \quad (2.17)$$

implying that up to a gauge transformation $a = A/r$. Substituting this in I_{eff} , we get an effective action for A only that describes a fractional quantum Hall effect:

$$I'_{\text{eff}} = \frac{1}{r}\text{CS}(A) = \frac{1}{r} \frac{1}{4\pi} \int_{M_3} d^3x \epsilon^{ijk} A_i \partial_j A_k. \quad (2.18)$$

Here $1/r$ appears where k usually does, and this suggests that the Hall conductivity in this model is $1/r$. That is correct. But there clearly is something wrong with the derivation because the claimed answer for the effective action $I'_{\text{eff}} = (1/r)\text{CS}(A)$ does not make sense as it violates gauge invariance. The mistake is that in general, as F may have a flux quantum of 2π , and f has the same allowed flux quantum (otherwise the action we assumed would not be gauge-invariant), for a given A it is not possible to solve the equation (2.17) for a . Thus, it is not possible to eliminate a from this system and give a description in terms of A only. The reason that “integrating out a ” gives the right answer for the Hall current is that this procedure is valid locally and this is enough to determine the Hall current. The system has more subtle properties (fractionally charged quasiparticles and topological degeneracies) that can only be properly understood in the description with a as well as A . An introduction to those properties will be given in Lecture Three.

2.4 Relation To Band Topology

Going back to a theory that can be described in terms of A only, we have then an integer k in the macroscopic description. But there is also an integer in the microscopic description of a band insulator, the TKNN invariant [11]. It arises as follows. We consider a crystal with N bands, of which n are filled. We assume the system is completely gapped, for all values of the momentum. As we learned yesterday, in a 2d system it is generic to have no band crossings.

We are in the same situation as in our discussion yesterday of Weyl semimetals, except that there are no band-crossing points, so we work over the whole Brillouin zone \mathcal{B} , without removing anything. As we are in two-dimensions, \mathcal{B} is a two-torus. At momentum p , let $\mathcal{H}_p \cong \mathbf{C}^N$ be the full space of all states, and \mathcal{H}'_p the subspace of filled levels. We can regard \mathcal{H}_p as a rank (or dimension) N “trivial bundle” over \mathcal{B} and \mathcal{H}'_p as a “subbundle” of rank n . The integer we want, which we will call k' , is the first Chern class $c_1(\mathcal{H}'_p)$, integrated over \mathcal{B} . In terms of the Berry connection \mathcal{A} on the filled bands that we discussed yesterday, whose curvature we call \mathcal{F} , this integer is

$$k' = c_1(\mathcal{H}'_p) = \int_{\mathcal{B}} \frac{\text{Tr } \mathcal{F}}{2\pi}.$$

The basic claim of TKNN is that k' , the flux of the Berry connection, is the same as k , the coefficient of the quantum Hall current. The original proof was based on literally just calculating the current from first principles in terms of a matrix element in the fermion ground

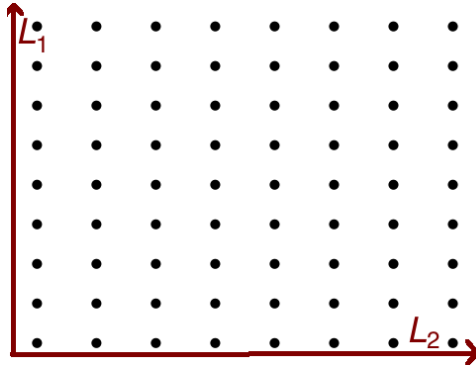


Figure 23: A periodic lattice of size $n_1 \times n_2$, with lattice constants a_1, a_2 in the two directions. The physical size of the lattice is $L_1 \times L_2$ with $L_1 = n_1 a_1$, $L_2 = n_2 a_2$.

state – which is written as an integral of single particle matrix elements over the Brillouin zone. I want to explain a different viewpoint that will emphasize that k' is not just a band concept but can be defined in the full many-body theory. (In Lecture Three, I will describe another approach essentially due to Haldane to the relation $k = k'$.)

We consider a finite sample, say on an $n_1 \times n_2$ lattice (fig. 23) for very large n_1, n_2 , where I will take lattice constants a_1, a_2 in the two directions. Thus the physical size of the lattice is $L_1 \times L_2$, with $L_1 = n_1 a_1$, $L_2 = n_2 a_2$. We assume periodic boundary conditions, maintaining the lattice translation symmetries. However, for the finite system, the momenta take discrete values

$$p_1 = \frac{2\pi s_1}{L_1}, \quad 0 \leq s_1 \leq n_1 - 1$$

$$p_2 = \frac{2\pi s_2}{L_2}, \quad 0 \leq s_2 \leq n_2 - 1.$$

The ground state of the finite system is of course obtained by filling all of the states in the first n bands with these values of the momenta.

Now, however, we turn on a background electromagnetic vector potential that is chosen such that the magnetic field vanishes, but an electron going all the way around the x_1 direction or the x_2 direction picks up a phase:

$$A_1 = \frac{\alpha_1}{L_1}, \quad A_2 = \frac{\alpha_2}{L_2}.$$

The phase picked up by an electron going around the x_1 (or x_2) direction is $\exp(i\alpha_1)$ (or $\exp(i\alpha_2)$) and up to a gauge transformation the range of these parameters is

$$0 \leq \alpha_1, \alpha_2 \leq 2\pi.$$

From the point of view of band theory, the effect of turning on the parameters α_1, α_2 is just to shift the momenta of the electrons, which become

$$p_1 = \frac{2\pi s_1 + \alpha_1}{L_1}, \quad 0 \leq s_1 \leq n_1 - 1$$

$$p_2 = \frac{2\pi s_2 + \alpha_2}{L_2}, \quad 0 \leq s_2 \leq n_2 - 1.$$

This actually shows that the spectrum is invariant under a 2π shift of α_1 or of α_2 (up to an integer shift of s_1 or s_2). For any α_1, α_2 , from the point of view of band theory, the ground state is found by filling all states in the first n bands with these shifted values of the momenta.

Now we think of the parameters α_1, α_2 as parameters that are going to vary adiabatically. Since they are each defined mod 2π , they parametrize a torus that I will call $\widehat{\mathcal{B}}$. ($\widehat{\mathcal{B}}$ can be viewed as a sort of rescaled version of the Brillouin zone \mathcal{B} .) Since Berry's construction is universal for adiabatic variation of parameters, we can construct a Berry connection $\widehat{\mathcal{A}}$ over $\widehat{\mathcal{B}}$, with curvature $\widehat{\mathcal{F}}$. $\widehat{\mathcal{A}}$ is a connection that can be used to transport the ground state as the parameters α_1, α_2 are varied. All we need to know to define it is that the ground state is always nondegenerate as α_1, α_2 are varied. We do not need to assume a single-particle picture (i.e. band theory). But I should say that for the conclusions we draw to be useful, at least in the form I will state, we need the gap from the ground state to be independent of L_1, L_2 as they become large. (Otherwise in practice our measurements in the lab may not be adiabatic. The stated assumption is not true for a fractional quantum Hall system, as we will discuss in Lecture Three.)

Using the Berry connection over $\widehat{\mathcal{B}}$, we can define an integer:

$$\widehat{k}' = \int_{\widehat{\mathcal{B}}} d\alpha_1 d\alpha_2 \frac{\widehat{\mathcal{F}}}{2\pi}.$$

But I claim that this is the same as the integer k' defined in band theory:

$$k' = \widehat{k}'.$$

The reason that this is useful is that the definition of \widehat{k}' is more general. To define k' , we assume band theory – that is, a single-particle description based on free electrons. The definition of \widehat{k}' assumes much less.

2.5 Proof Of The Equivalence

To understand why $k' = \widehat{k}'$, I have drawn in fig. 24 the discrete points in the Brillouin zone that obey the finite volume condition. The parameters α_1, α_2 parametrize one of the little rectangles in the picture, say the one at the lower left.

To compute k' , we integrate over \mathcal{B} , the full Brillouin zone. To compute \widehat{k}' , we integrate over the little rectangle, but for each point in the little rectangle, we sum over the corresponding shifted momenta. These are two different ways to organize the same calculation, so $\widehat{k}' = k'$.

So instead of proving the original TKNN formula $k = k'$, it is equivalent to prove that $k = \widehat{k}'$. This has the following advantage: \widehat{k}' is defined in terms of the response of the system to a changing electromagnetic vector potential A , so we can determine \widehat{k}' just from a knowledge of the effective action for A .

As practice, before determining the Berry connection for A , I am going to determine the Berry connection for an arbitrary dynamical system with dynamical variables $x^i(t)$. You can think of $x^i(t)$, $i = 1, \dots, 3$ as representing the position coordinates of a particle, but they really

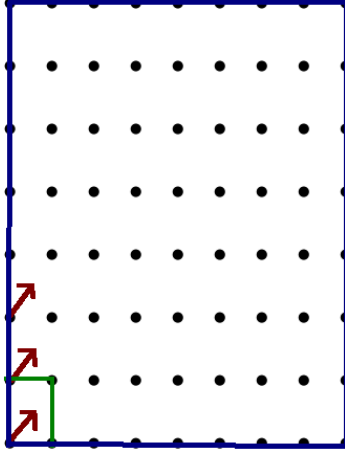


Figure 24: The large rectangle (in which opposite sides should be identified) represents the momentum space Brillouin zone \mathcal{B} that parametrizes the electron momentum. The small rectangle in the lower left (with again opposite sides identified) represents the macroscopic Brillouin zone $\widehat{\mathcal{B}}$ that parametrizes the shift angles α_1, α_2 . The black dots are the allowed values of the momentum for a finite lattice of size $n_1 \times n_2$ (drawn here for $n_1 = 8, n_2 = 7$). Turning on α_1 and α_2 shifts the allowed momenta as indicated by the arrows. In particular, the point at the lower left of the picture may be moved anywhere in the small rectangle that represents $\widehat{\mathcal{B}}$.

could be anything else (for example $x^i(t)$ could have $3N$ components representing the positions of N particles). Regardless, we assume an action

$$I = \frac{1}{2} \int dt g_{ij}(x) \frac{dx^i}{dt} \frac{dx^j}{dt} + \int dt \mathcal{A}_i(x) \frac{dx^i}{dt} - \int dt V(x) + \dots \quad (2.19)$$

(There might be higher order terms but it will be clear in a moment that they are not important.) We shall compute the Berry connection in the space of semiclassical states of zero energy, a condition that we satisfy by imposing the condition $V(x) = 0$. (This semiclassical approximation is valid in our problem because we do not need to treat the electromagnetic vector potential A quantum mechanically. We can view it as a given external field.)

Setting $V = 0$ means that we will evaluate the Berry phase not for all values of x but only for values of x that ensure $V(x) = 0$. So we drop the $V(x)$ term from the action, and only carry out transport in the subspace of the configuration space with $V = 0$. In adiabatic transport, we can also ignore the term

$$I_{\text{kin}} = \frac{1}{2} \int dt g_{ij}(x) \frac{dx^i}{dt} \frac{dx^j}{dt} \quad (2.20)$$

in the action, and any other term with two or more time derivatives. That is because if we transport from a starting point p to an ending point p' in time T , the derivative dx^i/dt is of order $1/T$, and $I_{\text{kin}} \sim 1/T$. In the adiabatic limit, $T \rightarrow \infty$ and this vanishes.

So the only term in the action that we need to keep is the term with precisely one time

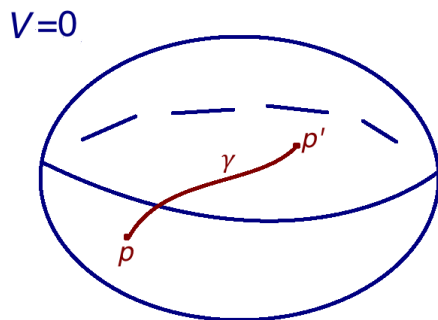


Figure 25: Propagation of a quantum particle between two points p and p' in the configuration space. We assume that the propagation occurs within the subspace with $V = 0$, represented here as a two-sphere. The propagating particle acquires a phase $\exp(iI/\hbar)$, where I is the classical action for the chosen trajectory.

derivative:

$$I' = \int dt \mathcal{A}_i(x) \frac{dx^i}{dt} = \int_p^{p'} \mathcal{A}_i(x) dx^i. \quad (2.21)$$

As I have indicated, this term depends only on the path followed from p to p' , and not on how it is parametrized. Now remember that the phase that a quantum particle acquires in propagating from p to p' along a given trajectory is $e^{iI/\hbar}$, where I is the action for that trajectory (fig. 25). For us, in units with $\hbar = 1$, this phase is just $\exp\left(i \int_\gamma \mathcal{A}_i dx^i\right)$.

But the connection which on parallel transport along a path γ gives a phase $\exp\left(i \int_\gamma \mathcal{A}_i dx^i\right)$ is just \mathcal{A} . What we have learned, in other words, is that for a system in which a quantum ground state can be considered to be equivalent to a classical ground state, the Berry connection is just the classical connection \mathcal{A} that can be read off from the classical action.

For the electromagnetic field in our problem, the action is

$$I = \frac{1}{2e^2} \int_{\mathbf{R}^{3,1}} d^3x dt \left(\vec{E}^2 - \vec{B}^2 \right) + \frac{k}{4\pi} \int_{W_3} d^2x dt \epsilon^{ijk} A_i \partial_j A_k + \dots \quad (2.22)$$

We assume, for example, periodic boundary conditions with very long periods L_1, L_2 in the two directions that are filled by our quantum Hall sample. (It doesn't matter if we assume periodic boundary conditions in the third direction.) A classical state of zero energy is labeled by the two angles α_1, α_2 that were introduced earlier. To compute the Berry phase, we are supposed to substitute this formula in the action and keep only the part of the action that has precisely 1 time derivative. This comes only from the Chern-Simons term.

After integration over x_1 and x_2 , the relevant part of the action is just

$$I' = -\frac{k}{2\pi} \int dt \alpha_1 \frac{d\alpha_2}{dt}. \quad (2.23)$$

From this, we read off the Berry connection

$$\nabla \equiv \left(\frac{D}{D\alpha_1}, \frac{D}{D\alpha_2} \right) = \left(\frac{\partial}{\partial\alpha_1}, \frac{\partial}{\partial\alpha_2} + i \frac{k\alpha_1}{2\pi} \right), \quad (2.24)$$

and hence the Berry curvature

$$\widehat{\mathcal{F}}_{\alpha_1\alpha_2} = -i \left[\frac{D}{D\alpha_1}, \frac{D}{D\alpha_2} \right] = \frac{k}{2\pi}. \quad (2.25)$$

(If we add to I' a total derivative term $\int dt \partial_t f(\alpha_1, \alpha_2)$, this will change the formula for ∇ but it will not change $\widehat{\mathcal{F}}$.)

We remember that the integer \widehat{k}' is supposed to be the integral of $\widehat{\mathcal{F}}/2\pi$ over the Brillouin zone. We can now compute

$$\widehat{k}' = \int_0^{2\pi} d\alpha_1 d\alpha_2 \frac{\widehat{\mathcal{F}}}{2\pi} = \int_0^{2\pi} d\alpha_1 d\alpha_2 \frac{k}{(2\pi)^2} = k. \quad (2.26)$$

Thus we arrive at a version of the famous TKNN formula: the coefficient k of the quantum Hall current can be computed as a flux integral of the Berry connection.

2.6 Edge States And Anomaly Inflow

Yesterday, we explained why a purely 1d quantum electron gas cannot have an imbalance between left-moving and right-moving electron excitations. As a reminder, the reason was that in a periodic orbit, “what goes up must come down” (fig. 2). From a field theory point of view, this is needed because right-moving gapless fermions without left-moving ones cannot be quantized in a gauge-invariant fashion. There is a 1+1-dimensional version of the Adler-Bell-Jackiw anomaly [6, 7].

However, one of the hallmarks of a quantum Hall system is that on its boundary it has precisely such an imbalance. The reason that this must happen is that when we verified the invariance of the Chern-Simons action

$$k\text{CS} = \frac{k}{4\pi} \int_{M_2 \times \mathbf{R}} d^3x \epsilon^{ijk} A_i \partial_j A_k \quad (2.27)$$

under a gauge transformation $A_i \rightarrow A_i + \partial_i \phi$, we had to integrate by parts. This integration by parts produces a surface term on the surface of our material – that is on $\partial M_2 \times \mathbf{R}$. There is no way to cancel this failure of gauge invariance by adding to the action a surface term supported on $\partial M_2 \times \mathbf{R}$. You can try to replace CS by

$$\text{CS} + \int_{\partial M_2 \times \mathbf{R}} dt dx (\text{????}), \quad (2.28)$$

where ????? is some polynomial in A and its derivatives, but whatever you try will not work. (I recommend this exercise.) It is precisely because the anomaly cannot be eliminated by adding some local interaction on the boundary that the anomaly is physically meaningful.

To cancel the anomaly, that is the failure of gauge invariance of CS along the boundary, requires the existence on the boundary of modes that are (1) gapless, so they cannot be integrated out to produce a local effective action for A only, and (2) “anomalous,” that is they are not possible in a purely 1-dimensional system. What fills the bill is precisely what we found does not exist in a purely 1-dimensional system: “chiral fermions,” that is right-moving gapless

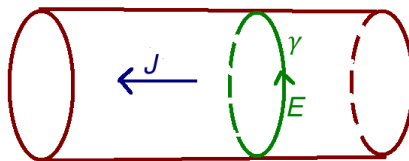


Figure 26: Sketched here is a quantum Hall system supported on the surface of an infinite cylinder. By varying $\oint_{\gamma} A \cdot d\ell$, where γ is the indicated contour, one can induce a current that goes “around” the cylinder. In a quantum Hall system, this will in turn induce an electric field “along” the cylinder, as indicated.

modes not accompanied by left-moving ones. The fact that an anomaly in the boundary theory can be canceled by the existence of a bulk interaction that is not gauge-invariant in the presence of a boundary is an illustration of the phenomenon of “anomaly inflow” [25].

Since the failure of k CS is proportional to k , the “chiral asymmetry” that is needed to cancel it is also proportional to k . In fact, the hallmark of an integer quantum Hall system with a Hall conductivity of k is precisely that

$$n_+ - n_- = k$$

where n_+ and n_- are the numbers of “right-moving” and “left-moving” gapless edge modes. Instead of giving a technical analysis of field theory anomalies to explain how this works, I will give a couple of possibly more physical explanations – one today and one in Lecture Three.

2.7 The Charge Pump

Today’s explanation involves a version of the Thouless charge pump [26]. Let us think of a quantum Hall system on the surface of a long cylinder. In fact for starters, think of an infinite cylinder (fig. 26).

We introduce the same sort of “twist parameter” α as before. We can imagine that there is a magnetic flux α through a solenoid inside the cylinder such that the magnetic field is 0 (or at least¹⁸ independent of α) in the cylinder itself but $\oint_{\gamma} A \cdot d\ell = \alpha$. Just as before, the parameter α is only gauge-invariant mod 2π .

We adiabatically increase α from 0 to 2π , with the scalar potential assumed to be 0. Since the electric field is then

$$\vec{E} = \frac{\partial \vec{A}}{\partial t}, \tag{2.29}$$

increasing α turns on an electric field that goes “around” the cylinder. But in the case of a quantum Hall system, this drives a current that is perpendicular to \vec{E} , in other words the

¹⁸In a conventional quantum Hall system, there is a strong magnetic field in the sample – that is in the cylinder – but we can assume it to be independent of α . In a topological band insulator with $k \neq 0$, the magnetic field can be assumed to vanish in the sample. The latter case is actually particularly natural for the discussion that follows.



Figure 27: A semi-infinite cylinder with a boundary at the left end.

current flows “along” the cylinder. The electrons therefore are pushed to the left (or right, depending on the sign of k).

An early explanation by Laughlin of the integer quantum Hall effect was the following. We assume that when $\alpha = 2\pi$, the system returns to the same state that it was in at $\alpha = 0$. (This assumption is not valid for fractional quantum Hall systems, as explained in section 2.9.) However, in the process, each electron may move k steps to the left, for some integer k . Notice that since the cylinder has a finite circumference S , the number of electrons per unit length is finite and thus it makes sense to say that each one moves k steps to the left, for some k . This was interpreted as the basic integrality of the integer quantum Hall effect. It does lead to the value $k/2\pi$ for the Hall conductivity.

Now let us consider a cylinder that is only *semi*-infinite, with a boundary at let us say the left end (fig. 27). The same parameter α as before makes sense, and we can still adiabatically increase it by 2π . Since a quantum Hall system is gapped, if we make a measurement far from the boundary, we will still see the same flux of valence electrons to the left as before, assuming that only valence bands (states below the fermi energy) are filled.

But what happens to the electrons when they arrive at the left boundary? A partial answer is that there are edge states, and electrons go from the valence bands to the edge states. But this is not enough: since the boundary has finite length, only finitely many electrons can go into edge states (of reasonable energy). What happens, at least in a topological band insulator (with finitely many bands) in which there is an upper bound on the possible energy of an electron, is that as electrons flow in to the left from the valence bands (the bands below the usual ε_F in the bulk) they must eventually flow back out to the right in the conduction bands (the bands above the usual ε_F). Moreover, all this is happening continuously in energy so it must be possible for an electron to evolve *continuously* from the valence bands in the bulk, to the conduction bands in the bulk, somehow passing through edge states.

2.8 Joining Valence And Conduction Bands

The spectrum must therefore look something like what is shown in fig. 28: there must be edge-localized states that can continuously leave the valence band, flow up through the Fermi energy, and eventually join the conduction bands. In the limit that the circumference S of the

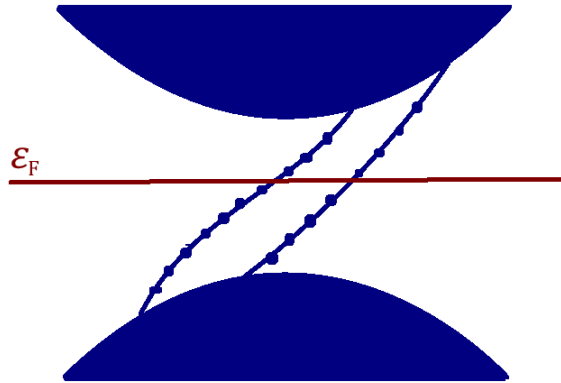


Figure 28: Drawn here is the $\varepsilon-p$ plane, where ε is the electron energy and p is the electron momentum along the boundary of a quantum Hall region. The solid regions are projections of the valence bands and conduction bands to the $\varepsilon-p$ plane. (In these projections, the component of electron momentum normal to the boundary is forgotten, as it is not a conserved quantity near the boundary.) Each curve in the figure represents a right-moving edge mode that connects the projection of the bulk valence bands to the projection of the bulk conduction bands. (In the case shown, there are two such curves, corresponding to $k = 2$.) Such a curve represents the energy-momentum relation of a family of edge-localized states; as in the discussion of Fermi arcs in Lecture One, such a curve terminates at a point where edge-localization breaks down and the edge-localized state becomes indistinguishable from a bulk state. The little beads represent, for some value of the parameter α , allowed values of the boundary momentum of an edge state when the circumference S of the boundary is finite.

cylinder becomes infinite, the edge-localized states have a continuous spectrum, but for finite S , they have a discrete spectrum, as shown in the figure. In the figure, each curve in the $\varepsilon - p$ plane that connects the valence bands to the conduction bands represents a right-moving edge mode. The little beads on the curve represent the allowed points on the curve for some large value of S . As we adiabatically increase α , each little bead moves up along the curve and under $\alpha \rightarrow \alpha + 2\pi$, each bead is shifted in position to the next one. So under $\alpha \rightarrow \alpha + 2\pi$, there is a net charge flow of 1 from the valence bands to the conduction bands for each right-moving edge mode.

Recall that as we discussed in Lecture One, a 1d mode is rightmoving if $d\varepsilon/dp > 0$ at $\varepsilon = \varepsilon_F$. A left-moving mode has $d\varepsilon/dp < 0$ at $\varepsilon = \varepsilon_F$, and under $\alpha \rightarrow \alpha + 2\pi$ produces a net charge flow of -1 from the valence band to the conduction band. Thus with n_+ and n_- as the numbers of right- and left-moving modes, the net charge flow under $\alpha \rightarrow \alpha + 2\pi$ is

$$k = n_+ - n_- . \tag{2.30}$$

It remains to tie up some loose ends in this explanation. The 1d edge modes cannot be defined on the whole 1d Brillouin zone of the boundary (which is a circle) because then we would be stuck with the fact that in a periodic orbit “what goes up must come down,” leading to $n_+ = n_-$. The asymmetry comes from branches of edge mode that exist in only a finite range of momenta $p_- \leq p \leq p_+$. What happens at the endpoints? The answer is the same as it was in the somewhat similar example of Fermi arcs that we discussed yesterday. The way that a family of edge-localized states can cease to exist at some momentum is by ceasing to be normalizable. This happens when the edge state becomes indistinguishable from a bulk state.

That is part of what makes it possible to have adiabatic transport from the valence bands (the states normally filled) to the conduction bands (the states normally empty), through the edge states. At the endpoint of the edge state spectrum, an edge state is indistinguishable from a bulk state.

For all this to make sense, adiabatic transport must remove as many electrons from the boundary in the conduction bands as approach the boundary in the valence bands. In other words, the total Hall conductivity of the empty (conduction) bands must be minus the Hall conductivity of the filled (valence) bands. That is actually a property of the Berry connection. Let \mathcal{A} be the usual Berry connection for the filled bands and \mathcal{F} the corresponding curvature; and similarly let \mathcal{A}' and \mathcal{F}' be the Berry connection and curvature of the empty bands. Then $\text{Tr } \mathcal{F} + \text{Tr } \mathcal{F}' = 0$, basically because for all bands together there is no Berry curvature. (The sum $(\text{Tr } \mathcal{F} + \text{Tr } \mathcal{F}')/2\pi$ would represent the first Chern class of all bands together, and this vanishes because all the electron states together form a trivial vector bundle over the Brillouin zone.)

Indeed, the Hall conductivities of filled and empty bands are respectively

$$\int_B \frac{\text{Tr } \mathcal{F}}{2\pi}, \quad \int_B \frac{\text{Tr } \mathcal{F}'}{2\pi} . \tag{2.31}$$

So the relation $\text{Tr } \mathcal{F} + \text{Tr } \mathcal{F}' = 0$ means that conduction and valence bands have opposite Hall conductivities, and in our thought experiment, the flow of “filled” states (i.e., states that would be filled in the ground state on an infinite cylinder) to the left equals the flow of “empty” states to the right.

2.9 More On The Fractional Quantum Hall Effect

I would like to next explain the assertion that a fractional quantum Hall system does not return to its previous state under $\alpha \rightarrow \alpha + 2\pi$. We will use the same macroscopic model of a fractional quantum Hall system that we used before in terms of the electromagnetic vector potential A and an emergent $U(1)$ gauge field a that only exists inside the material:

$$I_{\text{eff}} = \frac{1}{2\pi} \int_{M_3} d^3x \epsilon^{ijk} A_i \partial_j a_k - \frac{r}{4\pi} \int_{M_3} d^3x \epsilon^{ijk} a_i \partial_j a_k.$$

As in fig. 26, we consider a cylindrical sample and define $\alpha = \oint_\gamma A$. First let us discuss how to characterize the state of the system for a given α .

In principle, $\alpha = \oint_\gamma A$ can be controlled by varying the magnetic flux threaded by the cylinder. But there is an analogous parameter $\hat{\alpha} = \oint_\gamma a$ that cannot be controlled in that way. Just like α , $\hat{\alpha}$ is gauge-invariant mod 2π .

What can we say about $\hat{\alpha}$? Recalling that $F = dA$, $f = da$ are the ordinary electromagnetic field strength and its analog for a , the classical field equation for this system is

$$rf = F. \tag{2.32}$$

In the limit of an infinite cylinder, a can be treated classically. (We postpone the more interesting case of a finite cylinder until Lecture Three.) In the gauge $A_0 = a_0 = 0$, the equation $rf_{0i} = F_{0i}$ becomes

$$r \frac{da_i}{dt} = \frac{dA_i}{dt},$$

and therefore

$$r \frac{d\hat{\alpha}}{dt} = \frac{d\alpha}{dt}.$$

Hence when we adiabatically increase α by 2π , $\hat{\alpha}$ increases adiabatically by $2\pi/r$. Since $\hat{\alpha}$ is gauge-invariant mod 2π , the shift $\hat{\alpha} \rightarrow \hat{\alpha} + 2\pi/r$ does not return the system to its original state. We need to take $\alpha \rightarrow \alpha + 2\pi r$, and therefore the Hall conductivity can be smaller than its usual “quantum” by a factor of r .

Fig. 28 still has some sort of analog, but the edge states cannot be free electron states: They have to be capable of transporting a fractional charge under $\alpha \rightarrow \alpha + 2\pi$, and returning to their original state only under $\alpha \rightarrow \alpha + 2\pi r$.

2.10 More On Fermi Arcs

Finally, we will take another look at the Fermi arcs that we discussed in Lecture One. In Lecture One, we considered a model Hamiltonian that is valid near a generic band-crossing point and did an explicit computation to show the appearance of edge-localized states. However, the original paper [15] predicting these states did not proceed by solving a model Schrodinger equation. Rather the result was deduced as follows from some of the things that we have explained today.

First we recall the basic setup. Weyl points arise at special points in the Brillouin zone at which valence and conduction bands meet (fig. 10). Near a boundary of a finite sample, only two of the three components of momentum are conserved. So it is useful (fig. 17) to project the Brillouin zone and the band points in it to two dimensions, “forgetting” the component of

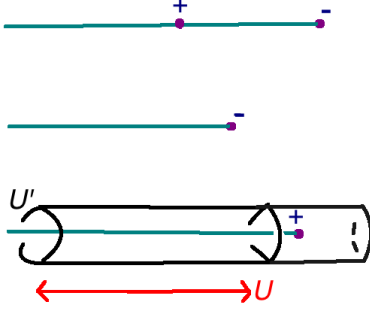


Figure 29: Projection of the bulk Brillouin zone to the boundary Brillouin zone that is appropriate for edge states. In the projection, the component of electron momentum normal to the boundary (here plotted horizontally) is forgotten. This component is parametrized by a circle U . In the figure, we have drawn another circle U' around the projection of one of the band-crossing points in the bulk. The product $U \times U'$ is a two-torus. This two-torus is used as the Brillouin zone of an auxiliary quantum Hall system that can be used in analyzing the Fermi arcs.

momentum that is not conserved. It is important to remember that in a crystal, the momentum components, including the component that is being “forgotten”, are periodic, and in particular the horizontal direction in the picture represents a circle $U \cong S^1$, though it is hard to draw this.

Now draw a little circle U' around the projection of one of the bad points, as in fig. 29. The product $U \times U'$ is a two-torus. We define an integer k^* as the Berry flux through $U \times U'$:

$$k^* = \int_{U \times U'} d^2p \frac{\text{Tr } \mathcal{F}}{2\pi}.$$

It receives a contribution of 1 or -1 for each positive or negative Weyl point enclosed by $U \times U'$. So in the example drawn, $k^* = 1$, but we would get $k^* = 0$ or $k^* = -1$ if we take U' to encircle one of the other two special points in the projection of fig. 29.

We have arranged so that the two-torus $U \times U'$ does not intersect any of the Weyl points. So the restriction to $U \times U'$ of the original 3d band Hamiltonian on the 3d Brillouin zone B is a gapped Hamiltonian H^* parametrized by a two-torus $U \times U'$. We can interpret H^* as the band Hamiltonian of some 2d lattice system that has a Hall conductivity of k^* . So as we have learned, H^* has edge modes, equal in number to k^* , that “bridge the gap” in energy between the filled and empty bands. This is sketched in fig. 30.

So there have to be edge states that intersect U' (the edge states are not labeled by U since U parametrizes the component of momentum that is not relevant to edge states). Since we had a lot of freedom in the choice of U' , the spectrum of edge-localized states has to consist of arcs that join the projections of band-crossing points.

The auxiliary 2d quantum Hall system that was used in this argument does not have any simple relation, as far as I know, to the 3d Weyl semi-metal that we are studying.

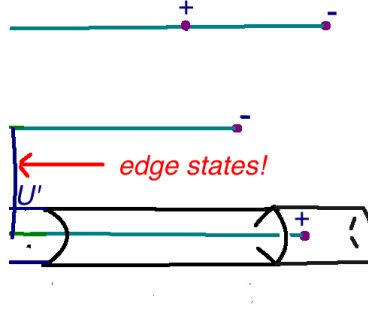


Figure 30: The band topology on $U \times U'$ is such that there must be edge states intersecting the circle U' and connecting the points in the boundary Brillouin zone that are projections of bulk band-crossing points with a nonzero net chirality.

3 Lecture Three

Today's lecture will concern three topics: (1) more on the fractional quantum Hall effect; (2) another explanation of the edge modes in the integer quantum Hall effect; (3) Haldane's model [23] of quantum Hall physics without an applied magnetic field.

3.1 More On The Fractional Quantum Hall Effect

As yesterday, we describe a fractional quantum Hall system macroscopically by an effective action for the electromagnetic vector potential A and an "emergent" $U(1)$ vector potential a that only exists inside the fractional Hall material. We can take the effective action to be the sum of the bulk Maxwell action

$$\frac{1}{2e^2} \int_{\mathbf{R}^{3,1}} d^3x dt \left(\vec{E}^2 - \vec{B}^2 \right) \quad (3.1)$$

plus a term that "lives" in the material:

$$I_{\text{eff}} = \int_{M_2 \times \mathbf{R}} d^2x dt \left(\frac{1}{2\pi} \epsilon^{ijk} A_i \partial_j a_k - \frac{r}{4\pi} \epsilon^{ijk} a_i \partial_j a_k \right). \quad (3.2)$$

For a first orientation, let us consider the interpretation of a "quasiparticle" that has a charge q under a . Here q must be an integer since a is a $U(1)$ gauge field. If such a quasiparticle is present at rest at a point $x = x_0$ in M_2 , then the part of the action that depends on a acquires an extra term and becomes

$$\int_{M_2 \times \mathbf{R}} d^2x dt \left(\frac{1}{2\pi} \epsilon^{ijk} A_i \partial_j a_k - \frac{r}{4\pi} \epsilon^{ijk} a_i \partial_j a_k \right) + q \int dt a_0(x_0, t). \quad (3.3)$$

The field equation for a_0 becomes

$$\frac{F_{12}(x)}{2\pi} - \frac{r f_{12}(x)}{2\pi} + q \delta(x - x_0) = 0. \quad (3.4)$$

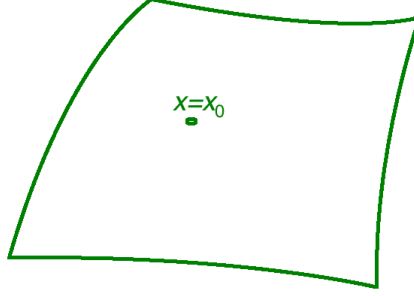


Figure 31: A flux tube of f in a two-dimensional surface. f vanishes except very near the point $x = x_0$, and has a nonzero integral.

To solve this equation, we obviously need a delta function in F_{12} and/or f_{12} . But which? In condensed matter, a delta function in f or F is really an idealization of a very tiny flux tube. Because a and f live only in two space dimensions, a delta function in f makes sense. It represents a little flux tube supported near the point x_0 in the two-dimensional surface M_2 (fig. 31). The coefficient of the delta function determines the integral of f over M_2 .

Because A lives throughout all of 3+1 dimensional spacetime, such a delta function does not make sense for $F = dA$. Of course, we can imagine a thin solenoid generating a flux tube of F , but this would extend into the third spatial dimension. It would not represent a quasiparticle that lives in M_2 . Alternatively, we could consider a small electric current loop in M_2 , say of small radius ρ . Such a current loop will create a magnetic dipole field in 3+1 dimensions. The magnetic field lines of a dipole form closed loops and there is no net flux through M_2 : if F is the dipolar magnetic field of a current loop then $\int_{M_2} F = 0$. (This is true whether or not the current loop is in M_2 .) So after coarse-graining, a small current loop will give 0, not a delta function in F .

So we have to solve the equation

$$\frac{F_{12}(x)}{2\pi} - \frac{r f_{12}(x)}{2\pi} + q\delta(x - x_0) = 0 \quad (3.5)$$

with a delta function in f_{12} and not in F_{12} , and hence near $x = x_0$,

$$\frac{f_{12}(x)}{2\pi} = \frac{q}{r}\delta(x - x_0). \quad (3.6)$$

Now if we go back to the action

$$I_{\text{eff}} = \frac{1}{2\pi} \int_{M_2 \times \mathbf{R}} d^2x dt \epsilon^{ijk} A_i \partial_j a_k - \frac{r}{4\pi} \int_{M_2 \times \mathbf{R}} d^3x \epsilon^{ijk} a_i \partial_j a_k, \quad (3.7)$$

we see that the charge density $J_0 = \delta I_{\text{eff}} / \delta A_0$ of A is

$$J_0 = \frac{f_{12}}{2\pi} = \frac{q}{r}\delta(x - x_0). \quad (3.8)$$

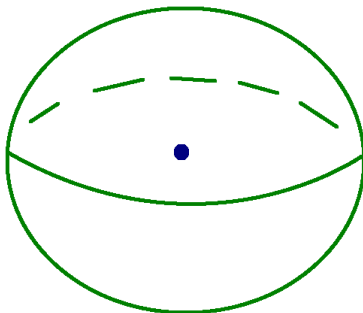


Figure 32: A spherical quantum Hall sample with a magnetic monopole inside. The Chern-Simons effective action predicts that if no quasiparticles are present, then the induced electric charge in the quantum Hall sample will equal k , the coefficient of the Hall conductivity. The system can be everywhere near its ground state if k is an integer, but if k is a fraction, then fractionally charged quasiparticles will inevitably be present.

Thus a quasiparticle with charge q for a has ordinary electric charge q/r (in units of the charge of the electron).

It is actually not necessary to go into so much detail to see that a fractional quantum Hall system must have fractionally charged quasiparticles. Return for a moment to an integer quantum Hall system:

$$I_{\text{eff}} = \frac{k}{4\pi} \int d^2x dt \epsilon^{ijk} A_i \partial_j A_k, \quad k \in \mathbf{Z}. \quad (3.9)$$

The corresponding electric charge density is

$$J_0 = \frac{\delta I_{\text{eff}}}{\delta A_0} = \frac{k F_{12}}{2\pi}. \quad (3.10)$$

If we place a magnetic monopole with one Dirac quantum

$$\int \frac{F_{12}}{2\pi} = 1 \quad (3.11)$$

inside a spherical sample (fig. 32), then the Chern-Simons effective action predicts that this induces in the material a charge

$$Q = \int_{M_2} J_0 = \int_{M_2} \frac{k F_{12}}{2\pi} = k, \quad (3.12)$$

and all is well if k is an integer. But if the effective value of k is not an integer, as in the case of the fractional quantum Hall effect, then there must be additional contributions to the electric charge in the form of fractionally charged quasiparticles that will appear somewhere on the surface of the material. Indeed, consider a thought experiment in which we start with an isolated magnetic monopole in vacuum. Then we bring in from infinity a large but finite collection of atoms and assemble them into a fractional quantum Hall system in the form of a large sphere surrounding the magnetic monopole, as in the figure. We can do this making

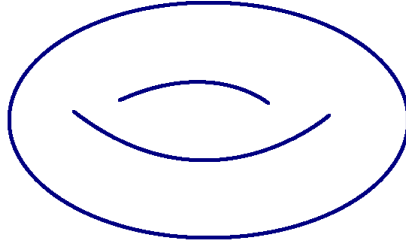


Figure 33: A two-dimensional torus.

sure that the atoms are always far away from the monopole. As electric charge is conserved and the vacuum is an insulator, the charge of the monopole does not change in this process. The total electric charge of the spherical quantum Hall sample that surrounds the monopole will be an integer, since this system is ultimately made from a finite number of electrons, protons, and neutrons, each of integer charge. The total electric charge of the system, however, will be the sum of the “bulk” contribution k of eqn. (3.12) and a further contribution from any quasiparticles that may be present. If k is not an integer, then the spherical quantum Hall system that surrounds a magnetic monopole will have to contain fractionally charged quasiparticles.

A full understanding of the fractional quantum Hall system requires treating a quantum mechanically. I will not attempt a complete explanation in this lecture, but will explain a few basic points.

First of all, part of the reason that we have gotten as far as we have without treating a quantum mechanically is that so far we considered a fractional quantum Hall system on an infinite or semi-infinite cylinder such as that of fig. 27, in which case a full quantum treatment is not necessary for many questions. For example, in section 2.9, we treated $\hat{\alpha} = \oint_{\gamma} a$ as an arbitrary constant, rather than a quantum variable. This is possible on an infinite or semi-infinite cylinder, but in the case of a compact sample we do need to treat a quantum mechanically.

In discussing the quantum mechanics of a , we will ignore A and just study the purely $2 + 1$ -dimensional problem:

$$I_{\text{eff}} = -\frac{r}{4\pi} \int_{M_2 \times \mathbf{R}} d^3x \epsilon^{ijk} a_i \partial_j a_k. \quad (3.13)$$

A noteworthy fact is that *there is no metric tensor in sight*, and therefore what we are trying to describe is a “topological quantum field theory.” It will describe not particle excitations, but only the “dynamics of the ground state(s)” and topological properties of quasiparticles. At long distances, many or most gapped quantum systems simply become trivial, and usually we take this for granted as the long distance behavior of a gapped system. But more generally a gapped quantum system can lead at long distances to a nontrivial topological quantum field theory, and that is what happens in the case of the fractional quantum Hall effect.

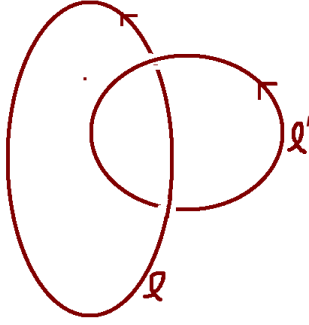


Figure 34: Linking of two loops in \mathbf{R}^3 .

A compact sample of nontrivial topology, such as the torus of fig. 33, is particularly interesting. We want to find the quantum states of the field a quantized on such a manifold.

The quantum states are supposed to make up a Hilbert space \mathfrak{H} . \mathfrak{H} is supposed to provide a representation of an algebra of quantum operators that is obtained, in some sense, by quantizing the space of classical observables. In a gauge theory, we consider only the gauge-invariant classical observables. So we should ask, “What are the gauge-invariant classical observables that we can make from a ?” As soon as we ask this question, we run into the following fact. A gauge-invariant local operator would have to be a polynomial in $f = da$ and its derivatives. But the classical field equation of a is

$$f = 0, \quad (3.14)$$

and therefore there are no local, gauge-invariant classical observables.

However, there *are* gauge-invariant “Wilson loop” operators. We pick a closed curve $\ell \subset M$ and define the “Wilson loop operator”

$$W_s(\ell) = \exp \left(is \oint_{\ell} a \right), \quad s \in \mathbf{Z}. \quad (3.15)$$

This operator is invariant under continuous deformations of ℓ . Here are two related explanations of this fact: (a) This is true because $f = 0$ so $W_s(\ell)$ can only see global information like Aharonov-Bohm phases; (b) More generally, in any topological quantum field theory, diffeomorphisms are symmetries and any loop ℓ is equivalent by diffeomorphism to any nearby loop to which ℓ can be deformed.

The physical meaning of the Wilson loop operator $W_s(\ell)$ is that the amplitude for a process in which a quasiparticle of charge s propagates around a loop ℓ is proportional to a factor of $W_s(\ell)$. If the loop ℓ can be continuously shrunk to a point without any singularity, then the operator $W_s(\ell)$ is trivial since the quasiparticle is not going anywhere. “Trivial” means that in this case $W_s(\ell)$ is equal to 1 as an operator. We are only interested in the case that this is not so.

There are two possible sources of Aharonov-Bohm-like phases that a Wilson loop operator $W_s(\ell)$ might see. There may be another similar operator $W_{s'}(\ell')$, where ℓ and ℓ' are “linked” and cannot be disentangled (fig. 34). (There will be a singularity if we try to pass ℓ through ℓ' .) This effect is associated to fractional statistics of the quasiparticles: It means that the presence

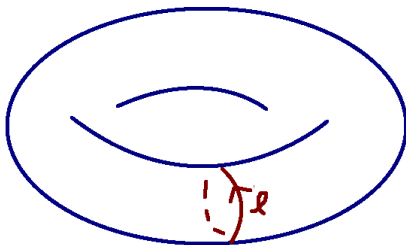


Figure 35: A noncontractible loop on a torus.

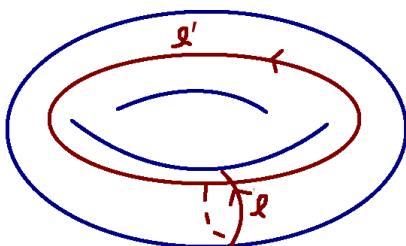


Figure 36: Two noncontractible loops on a torus that have a nonzero intersection number $\ell \cap \ell'$. In the example shown, the intersection number is 1.

of one quasiparticle propagating around ℓ' modifies the amplitude for a second quasiparticle to propagate around ℓ even if they are very far apart. Alternatively, and more like the classical Aharonov-Bohm idea, the loop ℓ might be “noncontractible” for topological reasons unrelated to the existence of other quasiparticles (fig. 35).

If two such loops ℓ and ℓ' on the torus have a nonzero intersection number $\ell \cap \ell'$ (fig. 36) then – as one can learn with the help of the classical Poisson brackets or quantum canonical commutators – the corresponding Wilson operators do not commute. They obey

$$W_s(\ell)W_{s'}(\ell') = \exp(2\pi i s s' \ell \cap \ell' / r) W_{s'}(\ell') W_s(\ell). \quad (3.16)$$

The basic case – sketched in the figure – is that $\ell \cap \ell' = 1$. Moreover, we may as well just set $s = s' = 1$ since $W_s(\ell)$ is just the ℓ^{th} power of $W_1(\ell)$ and similarly for $W_{s'}(\ell')$. If we set $A = W_1(\ell)$, $B = W_1(\ell')$, then the algebra obeyed by A and B is

$$AB = \exp(2\pi i / r) BA. \quad (3.17)$$

An irreducible representation of this algebra has dimension r , because

$$B \rightarrow ABA^{-1} = \exp(2\pi i / r) B \quad (3.18)$$

multiplies any eigenvalue of B by $\exp(2\pi i/r)$. So r states are needed to represent this algebra and actually r states are enough. These are the r “ground states of Chern-Simons theory on a torus,” for the case of the gauge group $U(1)$ at “level” r .

So this is the basis for the claim that *in the limit of a very large system*, a quantum Hall system on a topologically non-trivial manifold has a nontrivial vacuum degeneracy. The condition “in the limit of a very large system” is necessary, because the vacuum degeneracy is actually slightly lifted by exponentially small effects that result from quasiparticle tunneling around a noncontractible loop. Tunneling of a charge s quasiparticle around a noncontractible loop ℓ such as that of fig. 35 contributes to the effective Hamiltonian a term $W_s(\ell)$ with an exponentially small coefficient. (This coefficient is definitely not a topological invariant. It depends on the energy of the quasiparticle and the length of the loop ℓ – or more precisely the shortest length of a loop in its homotopy class, as this is the most likely tunneling path.)

3.2 More On Edge States Of The Integer Quantum Hall Effect

This completes our rather modest introduction to the vast topic of the fractional quantum Hall effect. Now we return to the integer quantum Hall effect. Largely following Haldane [23], we will give a conceptual, noncomputational proof of something of a fact that is familiar from Lecture Two (another conceptual explanation was already given in section 2.7): a $2 + 1$ -dimensional system with a Chern-Simons coupling in bulk

$$I_{\text{eff}} = \frac{k}{4\pi} \int d^3x \epsilon^{ijk} A_i \partial_j A_k, \quad (3.19)$$

and $n_+ - n_- = k$ chiral edge states on the boundary is completely consistent and anomaly-free. To do this, we will simply describe a physical realization. First we do this in a continuum language and then we do it via the Haldane model.

We couple the field A to a massive $2 + 1$ -dimensional Dirac fermion ψ of charge 1:

$$I_\psi = \int d^3x \bar{\psi} (\not{D} - m) \psi. \quad (3.20)$$

Since ψ is gapped, we can “integrate it out” and get a local effective action for A only. The dominant term at low energies turns out to be

$$\frac{\text{sign } m}{2} \text{CS}(A) = \frac{\text{sign } m}{2} \frac{1}{4\pi} \int d^3x \epsilon^{ijk} A_i \partial_j A_k. \quad (3.21)$$

The factor of $1/2$ is worrisome as it contradicts gauge invariance. However, we will always consider combinations in which it is absent. The factor $\text{sign } m$ follows from reflection symmetry (under which m and $\text{CS}(A)$ are both odd) and dimensional analysis.

The effective action $(\text{sign } m/2)\text{CS}(A)$ was first found [27, 28] from a Feynman diagram (fig. 37), and this is not a difficult calculation. However, in the spirit of the present lectures, it is more natural to get this result from the Berry flux.

We know that when any gapped system of charged fermions is “integrated out,” the resulting coefficient of $\text{CS}(A)$ equals the winding number of the momentum space Hamiltonian. The massive Dirac Hamiltonian in $2 + 1$ dimensions is

$$H = \sigma_x p_x + \sigma_y p_y + m \sigma_z. \quad (3.22)$$

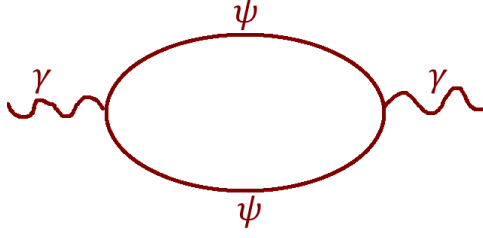


Figure 37: The one-loop Feynman diagram associated to the parity anomaly.

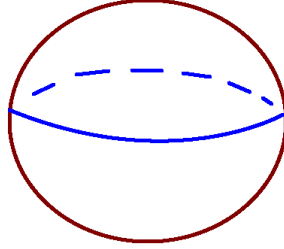


Figure 38: The equator of the two-sphere.

For large $|p|$, the mapping is

$$(p_x, p_y) \rightarrow \left(\frac{p_x}{\sqrt{p_x^2 + p_y^2}}, \frac{p_y}{\sqrt{p_x^2 + p_y^2}}, 0 \right), \quad (3.23)$$

which winds around the equator of the sphere (fig. 38).

The full mapping

$$(p_x, p_y) \rightarrow \left(\frac{p_x}{\sqrt{p_x^2 + p_y^2 + m^2}}, \frac{p_y}{\sqrt{p_x^2 + p_y^2 + m^2}}, \frac{m}{\sqrt{p_x^2 + p_y^2 + m^2}} \right) \quad (3.24)$$

has for its image the upper hemisphere or the lower hemisphere, depending on the sign of m (fig. 39). So the winding number is $\frac{1}{2}\text{sign } m$, and that is the Chern-Simons coefficient that we get by integrating out ψ .

For the moment, we want to consider a theory that is gapped and trivial at low energies, so along with ψ , we add a second fermion field ψ' of mass $-m$. This combination is trivial in the sense that the total Chern-Simons coefficient obtained by integrating out ψ and ψ' is

$$\frac{1}{2} (\text{sign } m + \text{sign } (-m)) = 0. \quad (3.25)$$

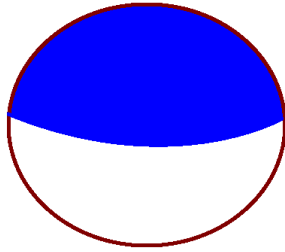


Figure 39: The upper hemisphere of the two-sphere.

There is no induced Chern-Simons coupling, so there is no anomaly on a manifold with boundary.

On a sample with boundary, we want a boundary condition such that the system remains trivial even along the boundary – no edge excitations at all. This will certainly be consistent and physically sensible! On a half-space $x_1 \geq 0$, what boundary condition will ensure that nothing happens along the boundary?

A boundary condition that does the trick is

$$\psi'|_{x_1=0} = \gamma_1 \psi|_{x_1=0}. \quad (3.26)$$

Recall that ψ and ψ' have equal and opposite masses

$$(\not{\partial} - m) \psi = 0 = (\not{\partial} + m) \psi', \quad (3.27)$$

and that in $2+1$ dimensions, the fermion mass is odd under reflection. So if we combine ψ and ψ' to a single fermion $\hat{\psi}$ defined on all of \mathbf{R}^3 by

$$\hat{\psi}(x_1, x_2; t) = \begin{cases} \psi(x_1, x_2; t) & \text{if } x_1 \geq 0 \\ \gamma_1 \psi'(-x_1, x_2; t) & \text{if } x_1 \leq 0, \end{cases} \quad (3.28)$$

then $\hat{\psi}$ just obeys

$$(\not{\partial} - m) \hat{\psi} = 0, \quad (3.29)$$

and certainly has no gapless mode.

Now, while keeping the fermion kinetic energy and the boundary conditions fixed, we change the sign of the mass of ψ' and take both ψ and ψ' to have the same mass $m > 0$. This cannot affect the consistency of the theory since the mass is a “soft” perturbation. Of course, when the mass of ψ' passes through zero, the theory becomes ungapped and passes through a phase transition. What is there on the other side of this transition? The Hall conductivity – that is the coefficient of $\text{CS}(A)$ in the effective action – is now $\frac{1}{2}(1+1) = 1$. By itself this would be anomalous. But the Dirac equation for $\hat{\psi}$ is now

$$(\not{\partial} - m \text{sign}(x_1)) \hat{\psi} = 0, \quad (3.30)$$

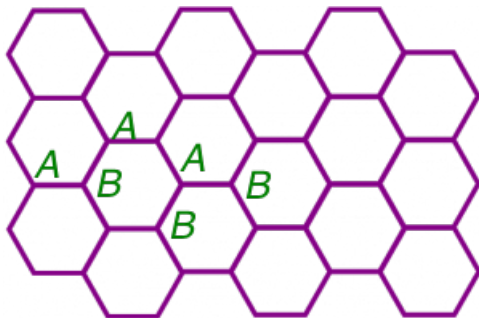


Figure 40: A hexagonal or honeycomb lattice. This is a bipartite lattice; lattice sites can alternately be labeled A or B in such a way that the nearest neighbors of A sites are B sites and vice-versa. The A sites are all equivalent under lattice translations and the same is true of the B sites. But there are no translation symmetries exchanging A and B sites. A unit cell, accordingly, contains one A site and one B site.

and thus the mass of $\widehat{\psi}$ changes sign in passing through $x_1 = 0$. As in a classic analysis by Jackiw and Rebbi [29], this change in sign of the mass leads to the existence of a gapless mode supported near $x_1 = 0$. The relevant solution is quite similar to what we have already seen in eqn. (1.59):

$$\psi = \exp(-m|x_1|)\psi_{\parallel}, \quad (3.31)$$

with

$$\gamma_1 \psi_{\parallel} = -\psi_{\parallel}, \quad \not{D}^{\parallel} \psi_{\parallel} = 0. \quad (3.32)$$

The condition $\gamma_1 \psi_{\parallel} = -\psi_{\parallel}$ determines ψ_{\parallel} to have definite chirality in the $1 + 1$ -dimensional sense, so what we get this way is a chiral edge mode that propagates along the boundary at $x_1 = 0$.

Thus we have a manifestly consistent construction of a $2 + 1$ -dimensional system that in bulk has an effective action $\text{CS}(A)$ (plus terms of higher dimension) and along the boundary has a chiral edge mode. Had we started with k pairs ψ, ψ' , we would have arrived in the same way at a bulk action $k\text{CS}(A)$ and k chiral edge modes. So we have confirmed the consistency of this combined system without having to investigate the “anomalies” of the chiral edge modes.

3.3 Haldane’s Model Of Graphene

It remains to describe how Haldane realized this system in a condensed matter model – a small perturbation of the standard band Hamiltonian of graphene. Graphene is an atomic monolayer of carbon atoms arranged in a hexagonal (or honeycomb) lattice, sketched in fig. 40. We think of this as a lattice in the $x - y$ plane, with z as the normal direction. A carbon atom has 6 electrons; 2 of them are in $1s$ states and 3 more go into forming covalent bonds with the 3 nearest neighbors of any given atom. (One can think of the electrons in these bonds as hybridized $2s$, $2p_x$, and $2p_y$ electrons.) We are left with 1 electron per atom, which is going to go into the $2p_z$ orbital – with spin up or down. Thus the two $2p_z$ orbitals will be “half-filled.”

The honeycomb lattice has two atoms per unit cell. Each unit cell has an A atom and a B atom, as explained in the figure. So the $2p_z$ orbitals form two bands (not counting spin) and we want to “half-fill” these bands.

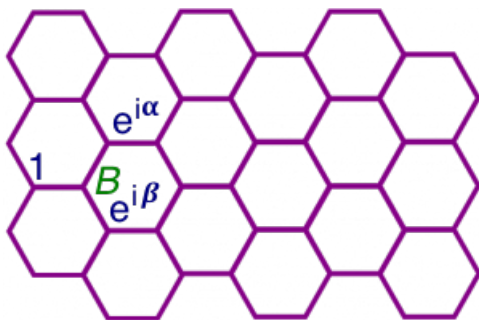


Figure 41: Hopping to a B site from its nearest neighbors.

What happens is dictated by symmetry up to a certain point, but the easiest way to understand it is to first solve a simple model [30, 31, 32] in which the Hamiltonian describes “nearest neighbor hopping” with amplitude t from the A -lattice to the B -lattice and vice-versa. A shortcut to write the momentum space Hamiltonian is as follows. Pick a point in the B lattice as shown in fig. 41, and let the momentum of an electron (and the normalization of its wavefunction) be such that the amplitudes at the three neighboring A points are 1 , $e^{i\alpha}$, and $e^{i\beta}$. Here α and β are arbitrary angles; they give a convenient parametrization of the Brillouin zone.

The total hopping amplitude to the indicated B site is then $1 + e^{i\alpha} + e^{i\beta}$ (times the hopping constant t). The Hamiltonian is hermitian, so the $B \rightarrow A$ hopping is the complex conjugate of this and the momentum space Hamiltonian is in the A, B basis

$$H = t \begin{pmatrix} 0 & 1 + e^{-i\alpha} + e^{-i\beta} \\ 1 + e^{i\alpha} + e^{i\beta} & 0 \end{pmatrix}. \quad (3.33)$$

H is traceless, so a band crossing occurs exactly when there is a zero-mode of H . To find such a zero-mode, we have to solve

$$1 + e^{i\alpha} + e^{i\beta} = 0, \quad (3.34)$$

with real α, β . The equation implies that $e^{i\alpha}$ and $e^{i\beta}$ are complex conjugates, and there are precisely two solutions

$$e^{i\alpha} = \frac{1}{2} (-1 \pm \sqrt{-3}) = e^{-i\beta}. \quad (3.35)$$

Expanding around either of these solutions, one finds a Dirac-like Hamiltonian, so we have found two “Dirac points” in the Brillouin zone.

This was a crude model, but the graphene lattice has a lot of symmetries. Apart from translation symmetries, the symmetries are as follows. As shown (fig. 42), let p be the center of one of the hexagons. Then one can rotate around p by any multiple of $2\pi/6$, and one can also reflect along various axes through p . For example, one can find a reflection that maps a given Dirac point to itself – and therefore (recall the discussion in section 1.9) ensures that the gapless Dirac modes that we found in the model remain gapless after any perturbation that preserves the reflection in question. One can also see that a $2\pi/6$ rotation exchanges the two Dirac points, ensuring that they are at the same energy.

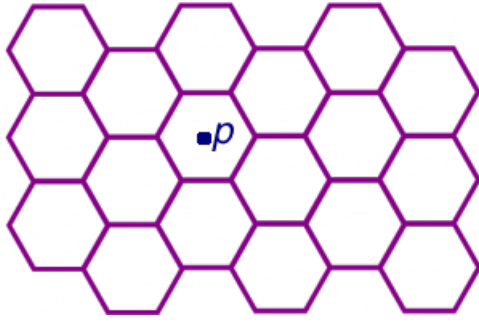


Figure 42: Apart from translation symmetries, the honeycomb lattice has a symmetry group of order 12. This can be identified as the group of all symmetries of the lattice that leave fixed a point p at the center of one of the hexagons. (Up to conjugation by the translation group, it does not matter which hexagon one picks.) The lattice has a symmetry group of order 6 consisting of rotations around p by an angle $2\pi n/6$, $n \in \mathbf{Z}$. Supplementing this with reflections that leave fixed a line through p gives the group of order 12.

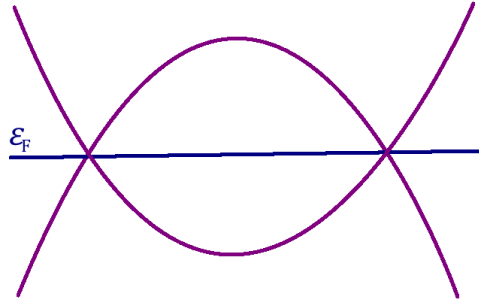


Figure 43: It is believed that the Fermi energy of an ideal graphene crystal in empty space, with spin-orbit forces turned off, precisely equals the energy of the Dirac points.

Furthermore, because (in the idealized hopping model) the band Hamiltonian is traceless away from the Dirac points, at every momentum away from the Dirac points, precisely one state has energy below the Dirac points and one has energy above them. So at half-filling, the Fermi energy is precisely the energy of the Dirac points. As discussed in section 1.6, this conclusion remains valid after any sufficiently small symmetry-preserving perturbations of the ideal Hamiltonian. It is believed to hold in the real world, for an ideal graphene crystal in empty space, with spin-dependent forces turned off (fig. 43).

In particular, it is believed that an ideal graphene crystal in the absence of spin-dependent forces has gapless Dirac-like excitations. Suitable perturbations involving symmetry breaking and/or spin-dependent forces can give a variety of gapped models. Haldane chose a perturbation that broke some symmetry and gave masses of the same sign to all Dirac modes. Allowing for spin, this gives a quantum Hall coefficient of $2 \times (1/2 + 1/2) = 2$. Kane and Mele [14] analyzed the effects of spin-dependent forces and arrived at the spin quantum Hall effect, the germ of a 2d topological insulator.

References

- [1] M. Z. Hasan and C. L. Kane, “Topological Insulators,” *Rev. Mod. Phys.* **82** (2010) 3045.
- [2] Xiao-Liang Qi and Shou-Cheng Zhang, “Topological Insulators And Superconductors,” *Rev. Mod. Phys.* **83** (2011) 1057-1110, arXiv:1008.2026.
- [3] M. Z. Hasan and J. E. Moore, “Three-Dimensional Topological Insulators,” arXiv:1011.5462, *Annu. Rev. Cond. Matt. Phys.* **2** (2011) 55.
- [4] B. A. Bernevig and T. L. Hughes, *Topological Insulators And Topological Superconductors* (Princeton University Press, 2013).
- [5] E. Witten, “Free fermions And Topological Phases,” arXiv:1508.04715.
- [6] S. Adler, “Axial Vector Vertex In Spinor Electrodynamics,” *Phys. Rev.* **177** (1969) 2426-2438.
- [7] J. S. Bell and R. Jackiw, “A PCAC Puzzle: $\pi^0 \rightarrow \gamma\gamma$ In The Sigma Model,” *Nuovo Cimento* **A60** (1969) 47-61.
- [8] C. Herring, “Accidental Degeneracy In The Energy Bands Of Crystals,” *Phys. Rev.* **52** (1937) 365-73.
- [9] H. B. Nielsen and M. Ninomiya, “A No-Go Theorem For Regularizing Chiral fermions,” *Phys. Lett.* **B105** (1981) 219.
- [10] D. Friedan, “A Proof Of The Nielsen-Ninomiya Theorem,” *Commun. Math. Phys.* **85** (1982) 481.
- [11] D. J. Thouless, M. Kohmoto, M. P. Nightingale, M. den Nijs, “Quantized Hall Conductance In A Two-Dimensional Periodic Potential,” *Phys. Rev. Lett.* **49** (1982) 405.
- [12] M. V. Berry “Quantal Phase Factors Accompanying Adiabatic Changes,” *Proc. Royal Soc.* **A392** (1802) 45-57.
- [13] P. Schuster and N. Toro, “Continuous-Spin Particle Field Theory With Helicity Correspondence,” *Phys. Rev.* **D91** (2015) 025023, arXiv:1404.0675.
- [14] C. L. Kane and E. J. Mele, “Quantum Spin Hall Effect In Graphene,” *Phys. Rev. Lett.* **95** (2005) 226801.
- [15] X. Wan, A. M. Turner, A. Vishwanath, and S. Y. Savrasov, “Topological Semimetal and Fermi-Arc Surface States in the Electronic Structure of Pyrochlore Iridates,” arXiv:1007.0016, *Phys. Rev.* **B83** (2011) 205101.
- [16] L. Fu, E. Mele, and C. Kane, “Topological Insulators In Three Dimensions,” *Phys. Rev. Lett.* **98** (2007) 106803, arXiv:cond-mat/0607699.

- [17] S. Murakami, “Phase Transition Between the Quantum Spin Hall and Insulator Phases in 3D: Emergence of a Topological Gapless Phase,” *New J. Phys.* **9** (2007) 356, arXiv:0710.0930.
- [18] L. Fu and C. L. Kane, “Topology, Delocalization via Average Symmetry and the Symplectic Anderson Transition,” *Phys. Rev. Lett.* **109** (2012) 246605, arXiv:1208.3442.
- [19] B.-J. Yang and N. Nagaosa, “Classification of Stable Three-Dimensional Dirac Semimetals with Nontrivial Topology,” arXiv:1404.0754, *Nature Communications* **5** (2014) 4898.
- [20] J. E. Avron, L. Sadun, J. Segert, and B. Simon, “Topological Invariants In Fermi Systems With Time-Reversal Invariance,” *Phys. Rev. Lett.* **61** (1988) 1329-32.
- [21] S. M. Young, S. Zaheed, J. C. Y. Teo, and C. L. Kane, “Dirac Semimetal In Three Dimensions,” *Phys. Rev. Lett.* **108** (2012) 140405.
- [22] S. M. Young and C. L. Kane, “Dirac Semimetals In Two Dimensions,” arXiv:1504.07977, *Phys. Rev. Lett.* **115** (2015) 126803
- [23] F. D. M. Haldane, “Model For A Quantum Hall Effect Without Landau Levels: Condensed Matter Realization Of The ‘Parity Anomaly,’ ” *Phys. Rev. Lett.* **61** (1988) 2016-8.
- [24] X.-G. Wen, “Topological Orders and Edge Excitations in FQH States,” *Adv. Phys.* **44** (1995) 405, arXiv:cond-mat/9506066.
- [25] C. G. Callan, Jr., and J. A. Harvey, “Anomalies And Fermion Zero-Modes On Strings And Domain Walls,” *Nucl.Phys.* **B250** (1985) 427.
- [26] D. J. Thouless, “Quantization Of Particle Transport,” *Phys. Rev.* **B27** (1983) 6083-7.
- [27] N. Redlich, “Parity Violation And Gauge Noninvariance of the Effective Gauge Field Action In Three Dimensions,” *Phys. Rev.* **D29** (1984) 2366.
- [28] A. Niemi and G. Semenoff, “Anomaly-Induced Fermion Fractionization And Effective Actions In Odd-Dimensional Spacetimes,” *Phys. Rev. Lett.* **51** (1983) 2077-80.
- [29] R. Jackiw and C. Rebbi, “Solitons With Fermion Number 1/2,” *Phys. Rev.* **D13** (1976) 3398.
- [30] P. R. Wallace, “The Band Theory Of Graphite,” *Phys. Rev.* **71** (1947) 622.
- [31] G. Semenoff, “Condensed Matter Simulation Of A Three-Dimensional Anomaly,” *Phys. Lett.* **53** (1984) 2449.
- [32] D. P. DiVincenzo and E. P. Mele, “Self-Consistent Effective Mass Theory For Intralayer Screening In Graphite Intercalation Compounds,” *Phys. Rev.* **B29** (1984) 1685-94.